

# Sand Transport by Unbroken Water Waves Under Sheet Flow Conditions

JOHN TROWBRIDGE

*Woods Hole Oceanographic Institution, Woods Hole, Massachusetts*

DONALD YOUNG

*U.S. Army Corps of Engineers, Los Angeles, California*

A model of wave-induced onshore sand transport and resulting topographical changes seaward of the break point on a sloping beach is presented, for the specific case in which the waves are random, normally incident, weakly nonlinear, and relatively long, the bottom boundary layer is fully turbulent, and sand transport occurs as sheet flow. The model consists of the following components: (1) a new empirical expression for sand transport as sheet flow, in which the instantaneous transport rate is directly proportional to the instantaneous bottom shear stress; (2) an expression for the mean bottom shear stress, based on a theoretical analysis of the bottom boundary layer; (3) a simple representation of the shoaling wave field, in which the local properties are described by linear long wave theory, the probability density function of the surface displacement is Gaussian, and the waves conserve energy flux as they shoal; and (4) the equation for conservation of sediment mass. Computations based on the model compare favorably with recently reported field measurements of the onshore motion of a long offshore bar.

## 1. INTRODUCTION

Water waves incident on a sand beach generate a variety of fluid motions, which can produce a spatially varying sediment transport field resulting in topographical changes. The literature addressing hydrodynamics, sediment transport and topographical evolution on beaches is very extensive (see, for example, the reviews by *Holman* [1983], *Bowen and Huntley* [1984], *Komar and Holman* [1986], and *Battjes* [1988]). Although several researchers have made significant progress in understanding beach hydrodynamics, and several have proposed interesting hypotheses and models addressing the interaction between hydrodynamics and topographical changes, sediment transport on beaches remains in general a poorly understood process.

This paper addresses sand transport by water waves under a specific set of idealized conditions. In the case considered, random, unbroken, normally incident, weakly nonlinear, relatively long waves propagate shoreward above a gently sloping sand bottom with straight, parallel depth contours. The motion is intense enough so that the bottom boundary layer is fully turbulent, and so that sand ripples are not present and sand moves in a very thin layer near the bottom (sheet flow conditions). Although specialized, this case is relevant to processes occurring on natural beaches. *Freilich and Guza* [1984] and *Elgar and Guza* [1985, 1986] showed that models developed for random, weakly nonlinear, relatively long waves describe quite accurately the observed shoaling of waves seaward of the break point on gently sloping natural beaches. Sand transport as sheet flow does not occur at all times or on every part of a beach, but it seems likely that many of the more important topographical changes on beaches occur under relatively severe conditions when sheet flow is present.

The purposes of this paper are to present a model of wave-induced sand transport and resulting topographical changes under the stated conditions, and to present a comparison of computations based on the model with field measurements. The model consists of four components. The first is a new empirical expression for sand transport under oscillatory sheet flow conditions, in which the instantaneous transport rate is directly proportional to the instantaneous boundary shear stress. This expression differs substantially from previous theoretical and empirical expressions for the rate of sand transport in an oscillatory flow [e.g., *Madsen and Grant*, 1976b; *Bailard*, 1981; *Kobayashi*, 1982]. An analysis of detailed laboratory measurements reported by *Horikawa et al.* [1982] supports the new empirical expression, and provides an estimate of the required constant of proportionality. The second component of the model is an expression for the mean bottom shear stress in a wave-induced flow field, based on a theoretical analysis of the bottom boundary layer. The analysis is less detailed than previous theoretical analyses of turbulent wave boundary layers (see review by *Grant and Madsen* [1986]), but it is more appropriate for the present purposes because it allows for tangential motion of the sand bottom. The third component of the model is a simple representation of the shoaling wave field, in which the lowest-order properties of the motion outside of the bottom boundary layer are described locally by linear long wave theory, the probability density function of the surface displacement is Gaussian, and the waves conserve energy flux as they propagate shoreward. Field measurements reported by *Guza and Thornton* [1980, 1985] indicate that this simple representation of the wave field is fairly realistic. The fourth component of the model is the equation for conservation of sediment mass. The model contains a single empirical constant, determined from the measurements reported by *Horikawa et al.* [1982].

The staff of the Coastal Engineering Research Center of the U.S. Army Corps of Engineers obtained the field measurements used in this paper, at the Field Research Facility in Duck, North Carolina. *Birkemeier* [1984] presented a

Copyright 1989 by the American Geophysical Union.

Paper number 89JC00546.  
0148-0227/89/89JC-00546\$05.00

summary and discussion of these measurements, and *Howd and Birkemeier* [1986] reported the measurement program in detail. Our comparison of model computations and field measurements focuses on a six-month period during which a prominent offshore bar moved a significant distance onshore [*Birkemeier*, 1984]. The agreement between model computations and measurements of topographical changes is good near the crest of the offshore bar, suggesting that the model represents realistically the sand transport processes that occurred near the crest during the period of onshore bar motion.

The calculations of topographical changes presented here differ in several respects from previous theoretical calculations of topographical evolution due to normally incident, non-reflecting waves [*Sunumura*, 1980; *Shibayama and Horikawa*, 1980; *Mizuguchi and Mori*, 1981; *Shibayama and Horikawa*, 1982; *Dally and Dean*, 1984; *Stive and Battjes*, 1984; *Stive*, 1986; *Nishimura and Sunumura*, 1986]. The present model applies specifically to the region seaward of the break point, while previous model studies have focused primarily on the region inside and just outside of the surf zone. The present model applies specifically to sand transport as sheet flow, while previous studies have typically treated the case of rippled beds, and some have ignored the question of bedforms entirely. The present model incorporates a random, rather than monochromatic, representation of the wave field seaward of the break point. Finally, the present model incorporates a systematic treatment of the bottom boundary layer.

The model presented here describes only sand transport due to a wave-induced mean bottom stress, and does not include a down-slope "shaking" effect due to the direct influence of gravity on the transport process [e.g., *Bailard and Inman*, 1981; *Bailard*, 1981; *Kobayashi*, 1982]. The model does not incorporate the effect of edge waves, which may be important in creating and altering topographical features that are approximately periodic in the alongshore direction (see reviews by *Holman* [1983]; *Bowen and Huntley* [1984]; and *Komar and Holman* [1986]). The model applies to gentle offshore topography, and consequently does not incorporate the effect of directly reflected incident waves, which may be important in producing shore-parallel, periodic bars [*Hunt and Johns*, 1963; *Carter et al.*, 1973; *Lau and Travis*, 1973; *Short*, 1975; *Heathershaw*, 1982; *Heathershaw and Davies*, 1984; *Mei*, 1985; *Benjamin et al.*, 1987]. In addition, the present model does not incorporate standing cross-shore infragravity waves, which may influence shore parallel bars, particularly in the inner part of the surf zone [*Symonds and Bowen*, 1984; *Sallenger and Holman*, 1987].

A brief consideration of typical scales is useful. Under conditions of interest in this paper, a typical water depth is 5 m, a typical wave period is 10 s, a typical root-mean-square surface displacement is 50 cm, a typical bottom slope is 0.01, and a typical mean sand grain diameter is 0.02 cm. The solution for shoreward propagating, linear, long waves over a locally horizontal bottom [e.g., *Dean and Dalrymple*, 1984] indicates that the corresponding wave length is approximately 70 m, and the root-mean-square horizontal velocity just outside of the bottom boundary layer is approximately 70 cm/s. Under these conditions, existing experimental results indicate that the unsteady bottom boundary layer is turbulent [*Jonsson*, 1980] and that the sand bottom moves in a sheet flow mode [e.g., *Shibayama and Horikawa*,

1982]. The moveable-bed roughness model of *Grant and Madsen* [1982] suggests that the thickness of the bottom boundary layer is of order 10 cm, and the experimental results of *Horikawa et al.* [1982] suggest that the thickness of the moving sand layer is of order 1 cm.

The remainder of the paper is organized as follows. Section 2 is a discussion of the instantaneous rate of sand transport under oscillatory sheet flow conditions. Section 3 is an analysis of the wave-induced flow field, resulting in an expression for the mean bottom shear stress. Section 4 addresses the mean transport rate and topographical changes. Section 5 describes the field data set, and section 6 presents a comparison of model computations and field measurements. Section 7 presents a summary and conclusions.

## 2. THE INSTANTANEOUS RATE OF SAND TRANSPORT

In his review article on coastal processes, *Horikawa* [1981] identified four modes of sand transport in an oscillatory flow. In order of increasing flow intensity, these modes are (1) bedload transport above a plane bed; (2) bedload and suspended transport above a rippled bed, with bedload transport dominating; (3) bedload and suspended transport above a rippled bed, with suspended transport dominating; and (4) sheet flow, in which sand ripples are not present, the bed is essentially plane, and sand moves in a thin layer very near the bed. The present discussion addresses only sheet flow conditions. The primary purpose of the discussion is to show that detailed laboratory measurements under oscillatory sheet flow conditions are consistent with a model in which the instantaneous transport rate is directly proportional to the instantaneous boundary shear stress. A secondary purpose is to show that detailed laboratory measurements under oscillatory sheet flow conditions are not consistent with previous simple models of the transport process.

### 2.1. Laboratory Measurements

Several early laboratory studies of sand transport in oscillatory flows exist (see summaries by *Madsen and Grant* [1976b], *Hallermeier* [1982], and *Nielsen* [1988]). Although the mode of transport is unclear in some cases, most of the early studies addressed relatively weak flows, in which sheet flow probably did not occur. The exception is *Manohar's* [1955] study, which included experiments in which sheet flow apparently occurred. *Manohar* used an oscillating tray in still water with a sediment trap in the center of the tray. *Madsen and Grant* [1976a] suggested that *Manohar's* measurements under sheet flow conditions were biased by complex flows and transport patterns in the neighborhood of the trap, and *Hallermeier* [1982] suggested that the acceleration of the oscillating tray had a significant effect on the results. For these reasons, the present discussion does not address *Manohar's* measurements.

Three recent laboratory studies of sand transport in an oscillatory flow addressed sheet flow conditions specifically. *Horikawa et al.* [1982] reported estimates of particle concentrations and velocities under sheet flow conditions in an oscillating water tunnel. Because of the symmetry of the water tunnel and the purely sinusoidal forcing flow, there was no mean transport in these experiments. *Horikawa et al.* used two measurement techniques. The first, used in the upper part of the transport field, was analysis of mo-

tion pictures, which provided estimates of particle velocities and concentrations. The second technique, used in the lower part of the transport field, where concentrations were large and the motion picture technique reportedly could not be used, was measurement of electronic resistance, which provided an indirect estimate of concentration. To determine particle velocities in the lower part of the transport field, Horikawa et al. used linear interpolation between the lowest measured velocity and the depth of no motion, assumed to be the highest location at which the concentration was equal to the concentration deep in the bed. Horikawa et al. used natural quartz beach sand with a mean grain diameter of 0.02 cm in water at room temperature. They reported ensemble-averaged particle velocities and concentrations as functions of elevation and the phase of the oscillatory flow in one case (Test 1-1), and they reported estimates of the mean of the absolute value of the transport rate in a total of six cases.

Sawamoto and Yamashita [1986] presented measurements very similar to those reported by Horikawa et al. [1982], based on the motion picture technique by itself. They reported the mean of the absolute value of the transport rate and the mean depth of motion for several sets of flow and sediment conditions. In one series of tests under conditions essentially identical to those used by Horikawa et al., Sawamoto and Yamashita found transport rates that were consistently smaller by a factor of approximately two. Determining which set of measurements is more accurate is difficult at this stage, but our opinion is that the measurements reported by Horikawa et al., although limited in scope and possibly subject to questions regarding experimental techniques, are more reliable. A plausible explanation for the discrepancy between the two sets of measurements is that the motion picture technique by itself cannot provide information about the lower part of the transport field, so that Sawamoto and Yamashita probably underestimated the transport rate. This explanation is consistent with the fact that Sawamoto and Yamashita reported depths of motion that were smaller by a factor of approximately two than the depths of motion observed by Horikawa et al. Because Sawamoto and Yamashita reported only the mean of the absolute value of the transport rate and the mean depth of motion, without information about the instantaneous transport rate, and because their measurements may have been biased, the present discussion does not address these measurements.

Ahilan and Sleath [1987] reported estimates of particle velocities under sheet flow conditions in an oscillating water tunnel, based on records from two closely spaced photodetectors. Because Ahilan and Sleath did not measure particle concentrations, their measurements cannot be used to estimate transport rates. Therefore, the present discussion does not address these measurements.

## 2.2. Existing Models

Several researchers have proposed simple expressions for the instantaneous rate of sand transport in an oscillatory flow. Of the more recent and commonly cited of these expressions, several may possibly be considered to apply to sheet flow conditions. Madsen and Grant [1976b] suggested a quasi-steady application of the empirical Einstein-Brown bedload transport formula, on the basis of a re-analysis of

early laboratory measurements. Most of the early measurements were carried out in relatively weak flows in which sheet flow probably did not occur. The applicability of the Einstein-Brown formula to intense flow conditions is therefore not clear, but Horikawa et al. [1982] suggested that it may apply to sheet flow conditions. Bowen [1980], Bailard and Inman [1981] and Bailard [1981] developed purely theoretical expressions for the sand transport rate in an intense oscillatory flow above a plane bed (presumably sheet flow conditions) based on Bagnold's [1963] energetics approach. Kobayashi [1982] developed a theoretical expression for the rate of bedload transport in an oscillatory flow, based on a simplified analysis of the forces acting on individual sand grains. Empirical support for this expression is limited to relatively weak flows, in which sheet flow probably did not occur, but the derivation does not seem to preclude its applicability to sheet flows. Recently, Ahilan and Sleath [1987] presented a detailed numerical model of sand transport under oscillatory sheet flow conditions, based on specific hypotheses about the manner in which stresses are transmitted inside of the bed. The complexity of this model is not consistent with the simpler approach adopted here, and the model of Ahilan and Sleath is not considered further in this paper. The model proposed by Madsen and Grant [1976b] is

$$q(t) = (40w_f d) \{ (f_w/2)U(t) | U(t) | / [gd(s-1)] \}^3 \quad (1)$$

Here  $q$  is the volume flux of sand per unit width,  $t$  is time,  $d$  is the mean grain diameter,  $w_f$  is the fall velocity of a spherical particle of sand with diameter  $d$ ,  $f_w$  is the wave friction factor,  $U$  is the free-stream velocity outside of the oscillatory boundary layer,  $g$  is gravitational acceleration, and  $s$  is the specific gravity of the sand. In this model, the wave friction factor has the value appropriate for a boundary roughness equal to the mean grain diameter. In the case of a horizontal bottom, the bedload transport model developed by Bailard and Inman [1981] is

$$q(t) = (f_w/2) \{ \epsilon_b / [g(s-1)\tan(\phi_o)] \} U^3(t) \quad (2)$$

and the suspended transport model developed by Bailard [1981] is

$$q(t) = (f_w/2) \{ \epsilon_s / [w_f g(s-1)] \} U(t) | U(t) |^3 \quad (3)$$

In (2) and (3),  $\phi_o$  is the angle of internal friction of the sediment, and  $\epsilon_b$  and  $\epsilon_s$  are empirical efficiency factors for bedload and suspended transport, respectively. The models developed by Bowen [1980] are very similar to the models developed by Bailard [1981] and by Bailard and Inman [1981], particularly in the case of a horizontal bed. In the limit in which flow conditions greatly exceed those required to initiate motion, which is appropriate for sheet flows, Kobayashi's [1982] expression approaches a form that is very similar in both magnitude and temporal variation to (2). All of the authors cited here recognized that there is in reality a phase shift between  $q$  and  $U$ , but set the phase shift equal to zero for the sake of simplicity.

A comparison of (1), (2) and (3) with measurements reported by Horikawa et al. [1982] in Test 1-1 is instructive. Figure 1 shows estimates of the transport rate as a function of the phase of the oscillatory flow, based on estimates of particle velocities and concentrations in Test 1-1. Figure 1 also shows the following equation:

$$q = A | \sin(\omega t + \phi) |^M \text{sgn}[\sin(\omega t + \phi)] \quad (4)$$

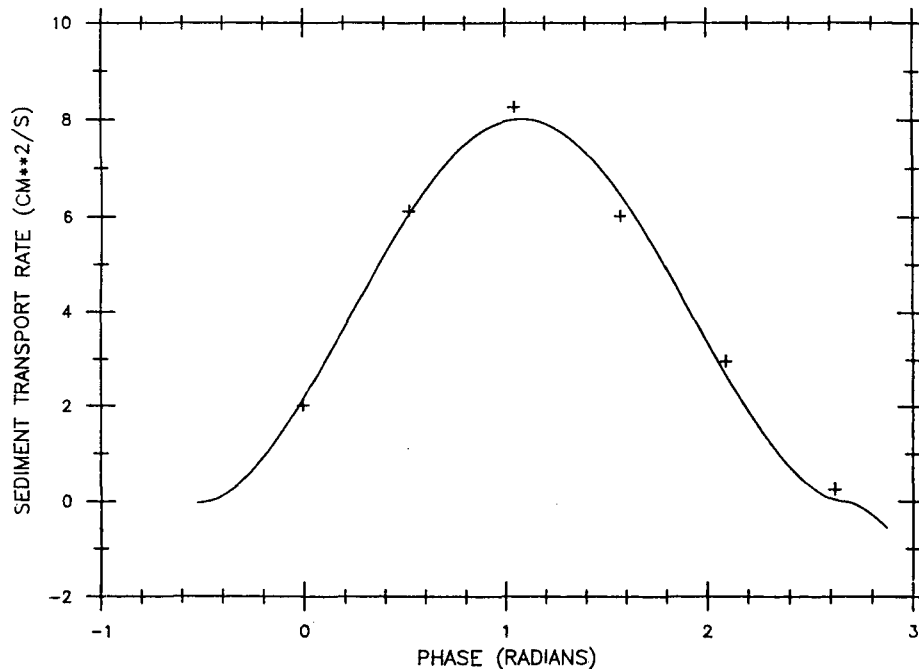


Fig. 1. Transport rate as a function of the phase of an oscillatory flow. Pluses: estimates based on laboratory measurements reported by Horikawa et al. [1982]. Solid line: equation (4) with least-squares estimates of  $A$ ,  $m$  and  $\phi$ .

Here  $\omega$  is the radian frequency of the flow, and  $A$ ,  $M$  and  $\phi$  are empirical constants determined by least-squares regression, based on an iterative linearization technique [Draper and Smith, 1966]. The free-stream velocity is proportional to  $\sin(\omega t)$ . Equation (4) is a reasonably general expression appropriate for a sinusoidal free-stream velocity, and is consistent with (1), (2) and (3). The least-squares estimates of the empirical constants and the corresponding 95% confidence intervals are

$$A = 8.0 \pm 1.0 \quad \phi = 0.49 \pm 0.09 \quad M = 1.7 \pm 0.6 \quad (5)$$

The confidence intervals are approximate because they are based on linearization of the nonlinear regression problem about the least-squares estimates of the constants. Bailard [1981] suggested adding (2) and (3) to determine the total transport, so that strictly speaking his model is not consistent with (4). For the present purposes, however, (2) and (3) may be considered separately.

Figure 2 shows calculations of the parameters  $A$  and  $M$  based on (1), (2) and (3), for the conditions in Test 1-1 reported by Horikawa et al. [1982] (maximum free-stream velocity equal to 127 cm/s,  $d = 0.02$  cm,  $s = 2.66$ ,  $\omega_f = 2.6$  cm/s,  $\phi_o = 37^\circ$ ). In the calculations for all three equations, the friction factor was 0.0062, which is appropriate for a boundary roughness equal to the mean grain diameter [Jonsson, 1966]. The bedload and suspended efficiency factors were 0.10 and 0.02, respectively, as suggested by Bailard [see Stive, 1986] for cross shore transport. Figure 2 also shows a cross section of the 95% confidence region in  $(A, M, \phi)$  space, determined by least-squares regression of (4) against the measurements shown in Figure 1. The confidence region is approximate because it is based on linearization of the nonlinear regression problem about the least-squares parameter estimates given in (5). The cross section shown in Figure 2 corresponds to  $\phi = 0.49$ , so that the cross section

is at the center of the confidence region. We chose this value because the models cited above correspond to  $\phi = 0$ , which is not realistic.

Figure 2 shows that (1), (2) and (3) produce results that differ significantly from the detailed measurements reported by Horikawa et al. [1982] in Test 1-1. The expression proposed by Madsen and Grant [1976b] reproduces the observed maximum transport rate (indicated by  $A$ ) quite accurately, but the temporal variation in this expression (indicated by  $M$ ) is very different from the observed temporal variation. Bailard's [1981] expression for suspended transport reproduces the maximum transport rate in Test 1-1 fairly accurately, in view of the uncertainty in the values of the required empirical efficiency factors, and the uncertainty in the value of the drag coefficient in the presence of a moveable bed. However, his expression for suspended transport indicates temporal variation that differs significantly from the observed temporal variation. More importantly, the expressions developed by Bailard and Inman [1981] and Bailard [1981] indicate that the bedload transport rate was almost an order of magnitude smaller than the suspended transport rate. In contrast, the detailed measurements [Horikawa et al., 1982] indicate that all of the transport occurred within about 1 cm of the rest level of the bed, and that the majority of the transport occurred below the rest level of the bed. The distinction between bedload and suspended load is unclear in this case, but the fact that the transport occurred so close to the bed suggests that (2) and (3) do not represent the transport processes accurately. One could justify increasing the friction factor in (2) by an order of magnitude to account for moveable-bed effects [Grant and Madsen, 1982], and one could perhaps justify neglecting suspended transport in the case of sheet flow. In this case, (2) would produce approximately the correct maximum transport rate. However, the temporal variation indicated by (2) differs significantly from the observed temporal variation.

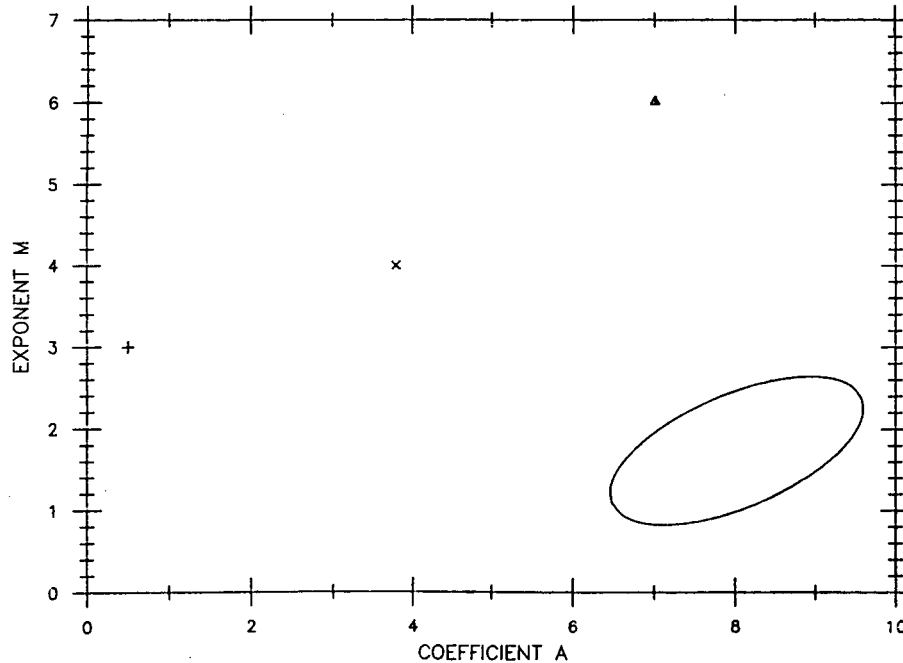


Fig. 2. The coefficients  $A$  and  $M$  in (4). Solid line: cross section of the 95% confidence region in  $(A, M, \phi)$  space, corresponding to  $\phi = 0.49$  rad, based on least-squares regression of (4) against the measurements in Figure 1. Triangle: calculation based on the model of *Madsen and Grant* [1976b]; plus: calculation based on the bedload transport model of *Bailard and Inman* [1981]; cross: calculation based on the suspended transport model of *Bailard* [1981]. All quantities are in cgs units.

### 2.3. A New Model

Experimental studies [e.g., *Jonsson and Carlsen*, 1976] and theoretical studies [*Lavelle and Mofjeld*, 1983; *Trowbridge and Madsen*, 1984] of oscillatory turbulent boundary layers above fixed rough surfaces indicate that in the case of a free stream velocity proportional to  $\sin(\omega t)$ , the bottom stress has the functional form indicated on the right side of (4), with an exponent  $M$  of slightly less than two and a phase shift  $\phi$  of approximately 0.5 rad. The fact that these values are close to the values determined from the measurements reported by *Horikawa et al.* [1982] suggests the hypothesis that under oscillatory sheet flow conditions, the instantaneous transport rate is directly proportional to the instantaneous boundary shear stress. The boundary shear stress may be considered to be the stress acting on the top of the moving layer of sand. The uncertainty in this location is not important for the present purposes, because the oscillatory turbulent boundary layer in the flow is much thicker than the moving layer of sand. Therefore, from the point of view of the flow, the sand bed approximates a moving, impermeable, plane surface at a fixed elevation.

A linear relationship between boundary shear stress and transport rate can be put into a dimensionally consistent form in several ways, and at present it is unclear which dimensionless variables are the most relevant. We have chosen the following dimensionally consistent form:

$$q(t)/(w_f d) = K \tau_b(t)/[\rho g d(s-1)] \quad (6)$$

Here  $\tau_b$  is the boundary shear stress,  $\rho$  is the density of the fluid, and  $K$  is an empirical dimensionless quantity, assumed here to be a constant. The normalization in (6) is the same as the normalization in the models proposed by *Madsen and Grant* [1976b] and by *Kobayashi* [1982], although the func-

tional form is quite different. As an alternative, we tested the normalization used by *Meyer-Peter and Mueller* [e.g., *Graf*, 1971], and found that the results presented below are not changed substantially.

Introduction of a quadratic drag law is necessary in order to use the measurements of the mean of the absolute value of the transport rate reported by *Horikawa et al.* [1982]. Although a quadratic drag law does not describe precisely the boundary shear stress in an oscillatory turbulent flow, it is sufficiently accurate for the present purposes. Equation (6) may therefore be written

$$q(t)/(w_f d) = K(f_w/2)U(t+T) |U(t+T)|/[gd(s-1)] \quad (7)$$

where  $T$  is the time shift by which the oscillatory free-stream velocity follows the oscillatory bottom stress. In the case of a sinusoidal free-stream velocity, the mean of the absolute value of (7) is

$$\langle |q| \rangle / (w_f d) = K(f_w/4)\bar{U}^2/[gd(s-1)] \quad (8)$$

where angular brackets denote a mean value and  $\bar{U}$  is the maximum value of  $U$ .

The difficulty with using (8) lies in evaluating the wave friction factor for a sand bed under sheet flow conditions. Here, we adopt the simple approach of treating the quantity  $Kf_w$  as a single empirical constant. This approach produces a better fit of the experimental results to (8) than using either the fixed-bed expression of *Jonsson* [1966] or the moveable-bed expression of *Grant and Madsen* [1982] to calculate the friction factor. Figure 3 shows  $\langle |q| \rangle / (w_f d)$  as a function of  $\bar{U}^2/[gd(s-1)]$ , based on the six cases reported by *Horikawa et al.* [1982]. The reasonably linear relationship between the two variables provides support for (8) and therefore for (6), although there is sufficient scat-

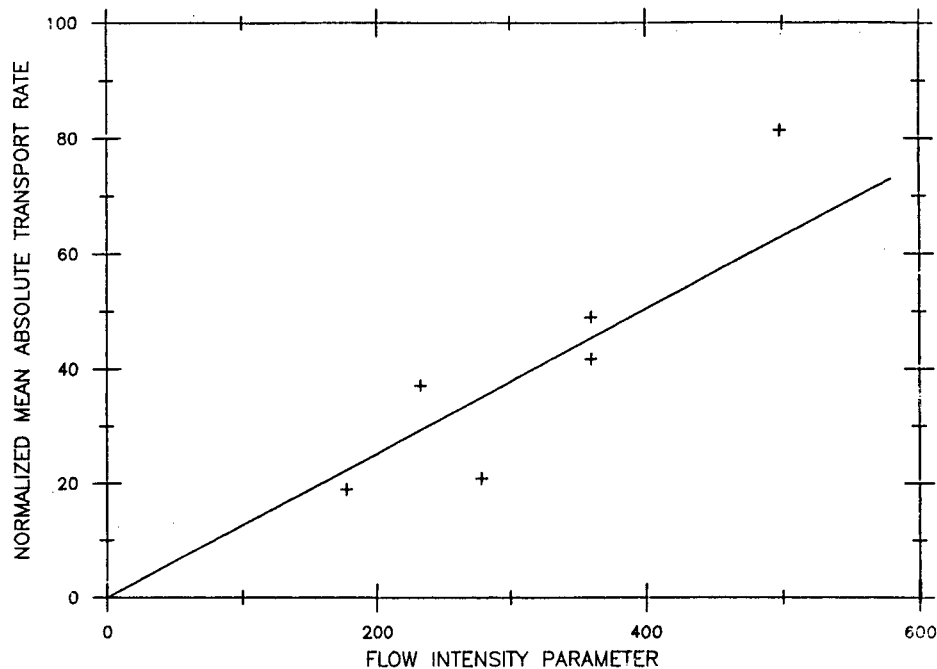


Fig. 3. Normalized mean of the absolute value of the transport rate,  $\langle |q| \rangle / (w_f d)$ , as a function of flow intensity parameter  $\hat{U}^2 / [gd(s-1)]$ . Pluses: measurements reported by Horikawa et al. [1982]. Solid line: best-fit line through the origin to the measurements.

ter so that the measurements do not verify definitely the functional form of the model. The best-fit value of  $Kf_w$  is  $0.50 \pm 0.14$  (95% confidence interval).

The quantity  $Kf_w$  is possibly not in reality a constant, and could, in particular, depend on mean grain diameter and the molecular viscosity of the fluid. Evaluation of the possible dependence of  $Kf_w$  on these quantities is not possible at present, because Horikawa et al. [1982] carried out experiments using only one type of sand in water at room temperature. At present it seems reasonable to use the above results, with the stated value of  $Kf_w$ , for transport problems involving quartz sand in water with mean grain diameters not too different from the mean grain diameter used by Horikawa et al. (0.02 cm).

Our interpretation of the measurements reported by Horikawa et al. [1982] differs substantially from their own interpretation, which was that the empirical Einstein-Brown formula, suggested by Grant and Madsen [1976b], represents the measurements fairly well. The reason for our different interpretation is that we examined both the instantaneous transport rate and the mean of the absolute value of the transport rate, while Horikawa et al. [1982] examined only the mean of the absolute value of the transport rate. The Einstein-Brown formula does in fact reproduce the measured mean of the absolute value of the transport rate fairly accurately, especially when the results are shown on a log-log plot with a wide parameter range, including all of the available measurements of sand transport in oscillatory flow (as in Horikawa et al. [1982]). As shown in Figure 2, however, the Einstein-Brown formula does not reproduce accurately the measured temporal variation of the transport rate.

The empirical expression proposed here for sand transport under oscillatory sheet flow conditions admittedly depends on a very limited number of laboratory measurements.

However, these measurements are, in our opinion, the most reliable that are currently available, and they are the only reported measurements that provide information about the instantaneous transport rate. Therefore, adoption of the simple transport expression proposed here is reasonable for the purposes of this paper.

### 3. THE MEAN BOTTOM SHEAR STRESS

Use of the empirical expression proposed in the previous section to calculate the mean rate of sand transport requires determination of the mean bottom shear stress. In the case considered in this paper, an expression for the mean bottom shear stress in terms of the local, low-order statistics of the wave field follows from an analysis of the mean momentum balance in the bottom boundary layer. The required analysis uses standard boundary layer approximations, and is an extension of an analysis presented by Longuet-Higgins [1958].

The mechanism producing a mean bottom shear stress is the following. The primary effect of the boundary layer is to shear the unsteady streamwise velocity within the layer. This in turn modifies the unsteady vertical velocity, because of the constraint of conservation of mass. At the outer edge of the boundary layer, the boundary layer modification to the unsteady vertical velocity is correlated with the unsteady streamwise velocity, so that there is a change in the mean flux of streamwise momentum across the top of the boundary layer. This change in the mean momentum flux must be balanced by a mean bottom shear stress, because there is nothing else that can balance it. The mean bottom shear stress turns out to be proportional to the mean rate of energy dissipation within the boundary layer, which can, at least in principle, be estimated based on previous results.

### 3.1. Governing Equations and Boundary Conditions

As stated in Section 1, the case considered is that of random, unbroken, normally incident, weakly nonlinear, relatively long waves propagating shoreward above a gently sloping sand bottom with straight, parallel depth contours. The bottom boundary layer is fully turbulent and the sand bottom moves in a sheet flow mode. The time scales for changes in the statistics of the incident waves and changes in the mean depth are much longer than the time scale of the waves themselves, so that for the purpose of analyzing the wave-induced stresses, we may consider the wave statistics and the mean depth to be independent of time. The motion then consists of a time-independent mean component, a fluctuating component associated with random waves, and a fluctuating component associated with turbulence. Conceptually, we may define a Reynolds average as a spatial average along a line parallel to the alongshore direction. The Reynolds-averaged motion includes the mean and "wave" components, but excludes the "turbulent" component. The Reynolds-averaged motion has no alongshore component and does not vary in the alongshore direction.

The equations governing the near-bottom flow are the boundary layer approximations to the two-dimensional, Reynolds-averaged, mass and momentum equations for an incompressible fluid. These are [e.g., Townsend, 1976]

$$\partial_x u + \partial_z w = 0 \quad (9)$$

$$\partial_t u + \partial_x(u^2) + \partial_z(uw) = \partial_t U + U \partial_x U + \partial_z(\tau/\rho) \quad (10)$$

Here the  $x$  axis is positive offshore, and coincides with the bottom, which may be considered locally plane. The  $z$  axis is perpendicular to the bottom and positive upward, and  $t$  and  $\rho$  are respectively time and density, as before. The Reynolds-averaged velocity vector in the  $(x, y, z)$  coordinate system is  $(u, 0, w)$ , the shear stress is  $\tau$ , and  $U$  is the value of  $u$  outside of the boundary layer, which may be considered independent of  $z$ . The first two terms on the right side of (10) represent the effect of the streamwise pressure gradient, which forces the flow in the boundary layer.

The boundary conditions at the outer edge of the layer are

$$\tau \rightarrow 0 \quad \text{and} \quad u \rightarrow U \quad \text{as} \quad z \rightarrow \infty \quad (11)$$

Here "infinity" implies in the usual boundary layer sense a distance much larger than the boundary layer thickness, but much smaller than the wavelength and water depth. Because the boundary layer is much thicker than the moving sand layer, and because the sand bottom is nearly plane under sheet flow conditions, it is reasonable to idealize the bottom as an impermeable, locally plane surface moving in its own plane. The corresponding bottom boundary condition is

$$w = 0 \quad \text{at} \quad z = 0 \quad (12)$$

where  $z = 0$  coincides with the top of the moving sand layer. In the present analysis,  $u$  is not required to be zero at the bottom because this condition is not necessary, and because it is not realistic for sheet flow conditions.

The leading terms in (10) are the first term on the left side, the first term on the right side, and the divergence of the shear stress. A straightforward order-of-magnitude analysis shows that the ratio of the advective terms to the

leading terms is of order  $a/h$ , where  $a$  is a representative wave amplitude and  $h$  is the local water depth. In weakly nonlinear waves,  $a/h$  is much smaller than unity. We therefore assume that the solution is expressible locally in a series of the following form:

$$u = u_1 + u_2 + \dots \quad (13)$$

with corresponding expressions for  $U$ ,  $w$  and  $\tau$ . Here the ratio of the second-order term  $u_2$  to the first-order term  $u_1$  is understood to be of order  $a/h$ , and subsequent terms are of higher order in  $a/h$ . Substitution of the series expressions into (9) and (10) yields at first order

$$\partial_x u_1 + \partial_z w_1 = 0 \quad (14)$$

$$\partial_t u_1 = \partial_t U_1 + \partial_z(\tau_1/\rho) \quad (15)$$

The second-order mass equation is not necessary for the present purposes. The second-order momentum equation is

$$\partial_t u_2 + \partial_x(u_1^2) + \partial_z(u_1 w_1) = \partial_t U_2 + U_1 \partial_x U_1 + \partial_z(\tau_2/\rho) \quad (16)$$

The straightforward perturbation procedure used here would not be appropriate for studying wave propagation over long distances or long times, because the cumulative effect of the small nonlinear terms does not remain small [e.g., Mei, 1982]. Locally, however, the nonlinear terms are small, and for the present purpose of examining the vertical structure of the mean momentum balance, a simple perturbation procedure is appropriate.

### 3.2. The Second-Order Mean Momentum Balance

By taking the mean of (15) and applying the boundary condition (11), one can show that at first order the mean bottom stress is zero. One must therefore consider the second-order momentum equation (16) in order to determine the mean bottom stress. By taking the mean of (16), and integrating the result from  $z = 0$  to an arbitrary fixed elevation  $z = \delta$  just outside of the boundary layer, where  $u$  is equal to  $U$  and  $\tau$  is zero, one obtains

$$\begin{aligned} \langle \tau_{b2}/\rho \rangle = & \delta \langle U_1 \partial_x U_1 \rangle - \partial_x \int_0^\delta \langle u_1^2 \rangle dz \\ & - \langle U_1 w_1 \rangle |_{z=\delta} \end{aligned} \quad (17)$$

where  $\tau_b$  is the bottom shear stress, as before, which may be expressed in a series of the form given by (13). The three terms on the right side of (17) are, respectively, the force on the boundary layer due to the mean pressure gradient, the cross-shore gradient of the mean momentum flux within the boundary layer, and the mean momentum flux across the top of the boundary layer.

To simplify (17), an expression for the vertical velocity  $w_1$  is necessary. By integrating the first-order mass-conservation equation (14) with respect to  $z$  and applying the bottom boundary condition (12), one obtains

$$w_1 |_{z=\delta} = -\delta \partial_x U_1 + \partial_x \int_0^\delta (U_1 - u_1) dz \quad (18)$$

Here we have used the facts that  $\delta$  is constant and  $U_1$  is independent of  $z$ . The first term on the right side of (18) is the first-order vertical velocity that would exist at  $z =$

$\delta$  if the boundary layer were not present. The final term is the modification produced by the boundary layer. It is important to note that this modification is nonzero not only inside of the boundary layer, but also at the outer edge of the boundary layer.

By substituting (18) into (17) and rearranging the result, one obtains

$$\begin{aligned} \langle \tau_{b2}/\rho \rangle = & \partial_x \int_0^\infty \langle U_1^2 - u_1^2 \rangle dz \\ & - \langle U_1 \partial_x \int_0^\infty (U_1 - u_1) dz \rangle \end{aligned} \quad (19)$$

The upper limit of the integrals has been set to infinity because the integrands vanish outside of the boundary layer. The force due to the mean pressure gradient does not appear in (19), because it is balanced by mean momentum fluxes. The first term on the right side of (19) is related to the momentum flux deficit produced by the boundary layer. The second term, which is more important for the present purposes, is the change in the mean momentum flux across the top of the boundary layer, caused by the boundary layer modification to the vertical velocity (see (18)).

### 3.3. Approximate Expression for the Mean Bottom Shear Stress

Until this point we have introduced no approximations beyond the boundary layer approximation and the series expansion ordered by  $a/h$ . In order to obtain a useful result, several additional approximations are necessary. The first is based on the fact that cross-shore changes in the mean properties of the wave-induced flow field, due to shoaling, energy dissipation and nonlinear processes, typically occur over distances much longer than the inverse wave number, under conditions of interest in this paper. Let  $k$  be a representative wave number, and let  $L$  be the cross-shore length scale for changes in the mean properties of the flow field. The first term on the right side of (19) is of order  $U(\Delta U)\delta/L$ , where  $\Delta U$  is the order of magnitude of the velocity defect in the boundary layer, and  $\delta$  is now the boundary layer thickness. The second term is of order  $U(\Delta U)\delta k$ . Because  $kL$  is much larger than unity, the second term is much larger than the first, and (19) becomes approximately

$$\langle \tau_{b2} \rangle \simeq \langle \rho U_1 \partial_x \int_0^\infty (u_1 - U_1) dz \rangle \quad (20)$$

With this approximation, the mean bottom shear stress is balanced solely by the change in the mean flux of momentum across the top of the boundary layer, caused by the boundary layer modification in  $w_1$  at the outer edge of the layer.

We can rewrite (20) as follows:

$$\begin{aligned} \langle \tau_{b2} \rangle \simeq & \partial_x \langle \rho U_1 \int_0^\infty (u_1 - U_1) dz \rangle \\ & - \langle \rho \partial_x (U_1) \int_0^\infty (u_1 - U_1) dz \rangle \end{aligned} \quad (21)$$

It can easily be shown that the second term on the right side is of order  $kL$  times the first, so that it is consistent with approximations introduced in (20) to approximate (21) by

$$\langle \tau_{b2} \rangle \simeq - \langle \rho \partial_x (U_1) \int_0^\infty (u_1 - U_1) dz \rangle \quad (22)$$

The following expression is an identity for arbitrary functions  $A(t)$  and  $B(t)$ :

$$\langle AB \rangle = \langle \partial_t (A \int B dt) \rangle - \langle \partial_t (A) \int B dt \rangle \quad (23)$$

If the process under consideration is stationary, the first term on the right side of (23) is zero. The lower limit of the integrals can easily be shown to be arbitrary, and the upper limit is understood to be  $t$ . Use of the identity (23) in (22) yields

$$\langle \tau_{b2} \rangle \simeq \langle \rho (\partial_x \int U_1 dt) \int_0^\infty \partial_t (u_1 - U_1) dz \rangle \quad (24)$$

By integrating the first-order momentum equation (15) from  $z = 0$  to an arbitrary elevation just outside the boundary layer, applying the boundary condition (11), and substituting the resulting expression into (24), we obtain

$$\langle \tau_{b2} \rangle \simeq - \langle \tau_{b1} \partial_x \int U_1 dt \rangle \quad (25)$$

This expression gives a relationship between the second-order mean bottom shear stress, the first-order bottom shear stress, and the first-order free-stream velocity.

We now assume that the first-order free-stream velocity  $U_1$  is governed by an equation of the following form:

$$\partial_t U_1 = (gh)^{1/2} \partial_x U_1 + \text{higher order terms} \quad (26)$$

so that the first-order motion outside the boundary layer behaves locally like an onshore-propagating, linear long wave. The higher order terms represent weak effects of frequency dispersion, shoaling, energy dissipation, and nonlinearity. Substitution of (26) into (25) and neglect of the higher order terms yields

$$\langle \tau_{b2} \rangle \simeq -(gh)^{-1/2} \langle \tau_{b1} U_1 \rangle \quad (27)$$

Equation (27) is similar to an expression obtained by Longuet-Higgins [1958], who analyzed a more idealized problem (spatially and temporally periodic monochromatic waves over a horizontal bottom). Kajima [1968] showed that the quantity  $\langle \tau_{b1} U_1 \rangle$  is equal to the time-averaged rate of energy dissipation in the bottom boundary layer. Equation (27) therefore shows that the mean bottom shear stress is proportional to the mean rate of energy dissipation. Because we expect the mean rate of energy dissipation to be positive, the mean bottom shear stress must be negative (i.e., onshore).

The problem of determining the mean bottom shear stress now reduces to estimating the rate of energy dissipation in the bottom boundary layer. There is considerable evidence that a simple quadratic drag law produces satisfactory estimates of the dissipation rate [e.g., Grant and Madsen, 1982], provided that one can estimate the drag coefficient accurately. We therefore assume that the first-order bottom shear stress and the first-order velocity outside of the boundary layer are related by a quadratic drag law, so that (27) becomes

$$\langle \tau_{b2} \rangle = -(f_w/2) \langle \rho U_1^2 | U_1 | \rangle (gh)^{-1/2} \quad (28)$$

where  $f_w$  is the friction factor, as before, and the phase shift between the first-order bottom stress and the first-order free-

stream velocity has been neglected. The effect of the phase shift is difficult to estimate in the case of random waves, but it is probably comparable to the corresponding effect in monochromatic waves, which would be to introduce a factor of  $\cos(\phi)$  into (28), where  $\phi$  is the phase shift (typically  $20^\circ$  to  $30^\circ$ ). The factor  $\cos(\phi)$  is sufficiently close to unity to be neglected in the present analysis. The difficult problem of estimating the friction factor under oscillatory sheet flow conditions need not be addressed for the present purpose of determining the mean rate of sand transport, as will be seen in the following section.

The solution for shoreward propagating linear long waves over a locally horizontal bottom gives the following approximate relationship between the first-order free-stream velocity and the first-order surface displacement  $\eta_1$ :

$$U_1 \simeq -(g/h)^{1/2} \eta_1 \quad (29)$$

Introduction of this expression is consistent with approximations introduced in (26), and is supported by field measurements reported by *Guza and Thornton* [1980], in relatively shallow water seaward of the break point on a gently sloping beach. Measurements reported by *Guza and Thornton* [1985] suggest that under conditions of interest here, the probability density function of the surface displacement is approximately Gaussian. If the probability density function is Gaussian, one can show straightforwardly that

$$\langle \eta_1^2 | \eta_1 \rangle = (8/\pi)^{1/2} \langle \eta_1^2 \rangle^{3/2} \quad (30)$$

Substitution of (29) and (30) into (28) yields

$$\langle \tau_{b2} \rangle \simeq -(2/\pi)^{1/2} f_w (\rho g/h^2) \langle \eta_1^2 \rangle^{3/2} \quad (31)$$

This is the desired expression for the mean bottom shear stress in terms of the local, low-order statistics of the wave field. In the following, we ignore the distinction between  $\langle \tau_{b2} \rangle$  and  $\langle \tau_b \rangle$ , because the first-order mean bottom shear stress is zero, and higher order terms are much smaller than the second-order term. Similarly, we ignore the distinction between  $\langle \eta_1^2 \rangle$  and  $\langle \eta^2 \rangle$ , because the first-order surface displacement contains most of the variance.

#### 4. THE MEAN TRANSPORT RATE AND TOPOGRAPHICAL CHANGES

##### 4.1. The Mean Transport Rate

By combining (6) and (31), one obtains

$$\langle q \rangle \simeq -(2/\pi)^{1/2} K f_w [w_f/(s-1)] \langle \eta^2 \rangle^{3/2} / h^2 \quad (32)$$

This is an expression for the mean rate of sand transport by random, unbroken, normally incident, weakly nonlinear, relatively long waves propagating shoreward above a gently sloping bottom with straight, parallel depth contours, for the case in which the wave-induced motion is intense enough so that the bottom boundary layer is turbulent and sand moves in a sheet flow mode. This expression gives the mean transport rate in terms of the properties of the sand, the local depth, and the variance of the surface displacement. The quantity  $K f_w$  has the value  $0.50 \pm 0.14$ , as determined in Section 2.

Equation (32) describes only one process (onshore sand transport due to a mean wave-induced bottom stress) and it applies only under a limited set of conditions. It does not incorporate several effects which may influence sand motion

on beaches, including down-slope shaking due to the direct influence of gravity on the transport process, formation of sand ripples, wave breaking, edge waves, and infragravity motions. The mean sand transport given by (32) is always onshore, and consequently this expression cannot describe, even as an approximation, an equilibrium configuration in which onshore transport by waves balances offshore transport by some other process, such as down-slope shaking. Equation (32) therefore applies only to conditions very far from equilibrium.

##### 4.2. Topographical Changes

Equation (32) may be used to calculate topographical changes seaward of the break point on a gently sloping sand beach, under circumstances in which sand transport by incident waves is the dominant process affecting topographical changes, and in which the special conditions required in the derivation are satisfied. In order to calculate topographical changes, (32) must be combined with a model of the shoaling wave field, and the equation for conservation of sediment mass.

The present analysis is based on the assumption that waves conserve energy flux as they propagate shoreward. This assumption is consistent with approximations made in the derivation of (31), and is supported by field measurements of unbroken waves on a gently sloping beach reported by *Guza and Thornton* [1980], which indicate that linear shoaling theory describes fairly accurately the cross-shore variation of the variance of the surface displacement. The energy flux associated with linear, long, normally incident waves is proportional to the following quantity [e.g., *Dean and Dalrymple*, 1984]:

$$F = (gh)^{1/2} \langle \eta^2 \rangle \quad (33)$$

The quantity  $F$  may vary gradually in time because of gradual temporal changes in the statistics of the incident waves, but it is independent of cross-shore position under the assumption of conservation of energy flux. Substitution of (33) into (32) yields

$$\langle q \rangle \simeq -(2/\pi)^{1/2} K f_w [w_f/(s-1)] g^{-3/4} F^{3/2} h^{-11/4} \quad (34)$$

This paper is limited to cases in which cross-shore variations in sediment properties do not contribute significantly to cross-shore variations in the mean transport rate. Under these circumstances, the mean transport rate given by (34) varies spatially only because of spatial depth variations.

In order to use the equation for conservation of sediment mass, it is convenient to divide the depth into two components:

$$h(x, t) = H(x, t) + \zeta(t) \quad (35)$$

Here  $H(x, t)$  is the depth of the bottom below a fixed datum, and  $\zeta(t)$  is the elevation of the mean sea surface above the same datum. The quantity  $H$  varies gradually in time because of topographical changes due to sand transport, and  $\zeta$  varies gradually in time because of low-frequency (for example, tidal and subtidal) changes in surface elevation. In reality,  $\zeta$  varies in space as well as time, but spatial variations are negligible over the relatively small distances of interest here. The mass conservation equation for sediment in the case of negligible alongshore variation is

$$(1-n)\partial_t H - \partial_x \langle q \rangle = 0 \quad (36)$$

where  $n$  is the porosity of the sand bed.

Substitution of (34) into (36) yields

$$\partial_t H - c\partial_x H \simeq 0 \quad (37)$$

where

$$c = (11/4)(2/\pi)^{1/2} [Kf_w/(1-n)][w_f/(s-1)] F^{3/2} g^{-3/4} h^{-15/4} \quad (38)$$

Equations (37) and (38) are similar to equations describing propagation of kinematic flood waves in long rivers [Lighthill and Whitham, 1955]. A straightforward analysis of these equations shows that, according to this model, a depth contour corresponding to a given value of  $H$  propagates onshore at a speed  $c$  that depends on  $H$  and on time, through temporal variations in  $F$  and  $\zeta$ . The propagation speed  $c$  decreases as the depth increases. In the case of an offshore bar, for example, this model predicts onshore propagation of the bar, accompanied by steepening of the landward slope and flattening of the seaward slope, without changes in the elevation of the crest of the bar. The model cannot describe the formation or destruction of an offshore bar.

If  $c(H, t)$  and  $X(H, t)$  are respectively the propagation speed and cross-shore position of a depth contour corresponding to a particular value of  $H$ , then

$$X(H, t) = X(H, 0) - \int_0^t c(H, \xi) d\xi \quad (39)$$

where  $\xi$  is a dummy variable of integration. Evaluation of the integral in (39) is straightforward, given time series of  $F$  and  $\zeta$ . By evaluating (39) for several values of  $H$ , one can construct a picture of topographical evolution on a beach. Like equation (32), equations (37), (38) and (39) apply only under circumstances in which onshore sand transport by incident waves is the dominant process affecting topographical changes, and the special conditions required in the derivation are satisfied.

#### 4.3. Qualitative Effects of Infragravity Motions and Down-Slope Shaking

Two effects not included in the model that may have an important effect on sand transport and topographical changes, even under the idealized conditions addressed in this paper, are infragravity motions and down-slope shaking due to the direct effect of gravity on the transport process. The possible role of infragravity motions is difficult to assess. Guza and Thornton [1985] presented field measurements on a gently sloping beach indicating that seaward of the break point, the velocity variance in the infragravity band is much smaller than the velocity variance in the incident wave band. This result suggests that infragravity motions do not have a significant effect under conditions considered here, which include only unbroken waves. On the other hand, if an offshore bar is present, theoretical work [e.g., Foda and Mei, 1981] shows that unbroken incident wave groups may resonate low-frequency trapped motions over the offshore bar. These trapped motions could produce a mean transport field resulting in significant topographical changes, resulting, for example, in creation or destruction of an offshore bar. It is difficult at present to determine the extent to which such motions, if present, influence topographical changes. The

question of the possible role of these motions must be reserved for future research.

It is possible to address the possible role of down-slope shaking in a more definite, although still qualitative, manner. This process is particularly relevant because it has been invoked in previous theoretical treatments of beach processes [e.g., Bailard and Inman, 1981; Holman and Bowen, 1982] as a mechanism by which a beach may reach an equilibrium configuration. For the purpose of the present discussion, the mean transport rate may be written

$$\langle q \rangle = Q_1 + Q_2 \quad (40)$$

where  $Q_1$  is the mean onshore transport rate due to the wave-induced mean bottom stress, given by (34), and  $Q_2$  is the offshore transport rate due to down-slope shaking. According to (34),  $Q_1$  has the following functional form:

$$Q_1 = Q_1(h, F) \quad (41)$$

where the symbols have the same meaning as before. It is reasonable to assume for the present purposes that  $Q_2$  has the following slightly different form:

$$Q_2 = \Gamma(h, F)\partial_x H \quad (42)$$

where  $\Gamma$  is a positive function of the arguments indicated. For example, the models of Kobayashi [1982] and Bailard [1981] for the down-slope shaking effect, if combined with assumptions that linear long wave theory is valid locally and energy flux is conserved, result in expressions of the form given in (42), for the case of a small bottom slope. By substituting (40), (41) and (42) into the mass conservation equation (36) one obtains

$$\partial_t H = c(h, F)\partial_x H + \partial_x [\gamma(h, F)\partial_x H] \quad (43)$$

where

$$c(h, F) = (1-n)^{-1}\partial_h Q_1(h, F) \quad (44)$$

$$\gamma(h, F) = (1-n)^{-1}\Gamma(h, F) \quad (45)$$

According to this formulation, down-slope shaking introduces a diffusion term into the equation governing topographical changes. In contrast to (37), (43) may have an equilibrium solution in which a bottom slope exists and the mean transport rate is everywhere zero. As in (37), however, the speed  $c$  remains positive, indicating onshore propagation. In order to obtain offshore propagation, one must incorporate other effects, such as formation of sand ripples, or wave breaking.

An analysis of topographical changes near the crest of an offshore bar demonstrates the qualitative effect of down-slope shaking in a particular case. By definition,  $\partial_x H$  is zero at the crest. The assumption that the curvature of the bottom reaches a relative maximum at the crest, so that  $\partial_x^2 H$  is also zero at the crest, simplifies the analysis and does not affect the qualitative conclusions. With this assumption, the depth  $H$  may be written

$$H(x, t) = H_C(t) + (1/2)[x - X_C(t)]^2 H_C''(t) + O[(\delta x)^4] \quad (46)$$

where  $X_C(t)$  is the position of the crest,  $\delta x$  is  $x - X_C$ , primes (') denote differentiation with respect to  $x$ , and a subscript  $C$  denotes evaluation at the crest. By substituting (46) into (43), (44) and (45) and expanding the results in Taylor series, one obtains, after straightforward algebra,

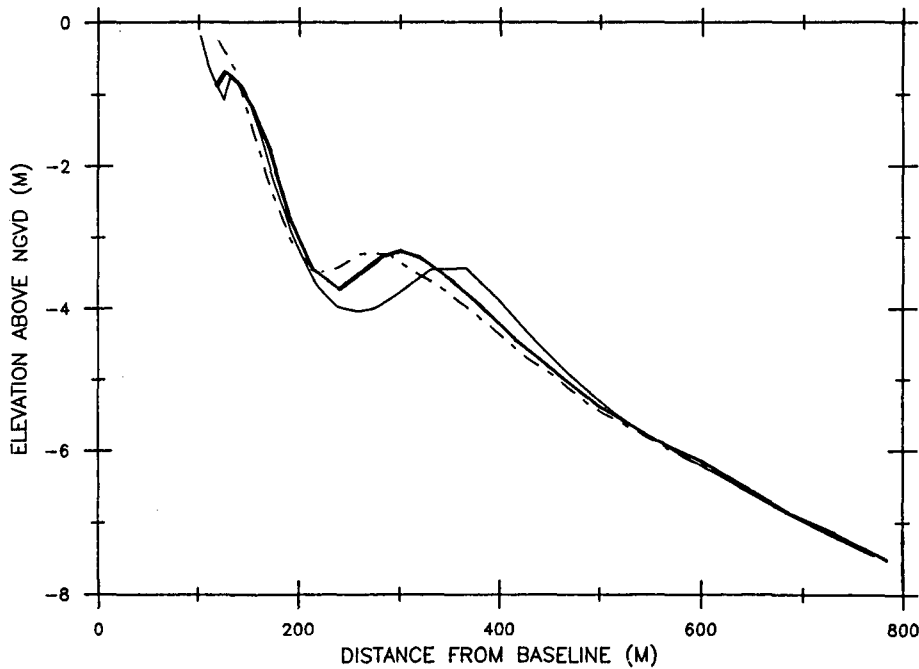


Fig. 4. Representative beach surveys along line 188 (see Figure 6) showing slow onshore motion of a long offshore bar. Light solid line: February 24, 1982; heavy solid line: May 17, 1982; dashed line: August 24, 1982. NGVD is National Geodetic Vertical Datum.

$$\partial_t H_C = \gamma(H_C + \zeta, F) H_C''(t) \quad (47)$$

$$\partial_t X_C = -c(H_C + \zeta, F) \quad (48)$$

In general,  $H_C''$  is positive. Equation (47) shows that the qualitative effect of down-slope shaking, as modeled here, is to increase the depth at the crest, which would remain constant if down-slope shaking had no effect. According to (48), the increasing depth at the crest in turn reduces the speed at which the crest propagates onshore, because  $c$  decreases as the depth increases.

A similar analysis of contours other than the crest of an offshore bar shows that down-slope shaking produces a slope-dependent modification to the onshore propagation speed.

## 5. THE FIELD DATA SET

The high-quality simultaneous measurements of beach topography, waves and tides presented by *Birkemeier* [1984] and reported in detail by *Howd and Birkemeier* [1986] provide a good opportunity to evaluate the model presented in the preceding sections. Our use of these measurements focuses on a six-month period between February and August 1982, during which an offshore, shore-parallel bar with a cross-shore length of about 200 m and a height of about 1 m moved about 100 m toward shore. According to *Birkemeier's* [1984] account, the bar was created during severe fall and winter storms, and the onshore motion of the bar occurred after the most severe storms, during a period in which the bar was usually well outside of the surf zone. Figures 4 and 5 show representative sequential surveys along two cross-shore lines separated by about 100 m in the alongshore direction. These figures show the slow onshore motion of the long offshore bar, and they show that the topography in the neighborhood of the offshore bar was approximately uniform

in the alongshore direction. A much shorter nearshore bar is also evident in Figures 4 and 5, but this was typically inside or near the surf zone and is beyond the scope of the present study. We chose the segment of the data set indicated in Figures 4 and 5 because the slow onshore motion of the long offshore bar was one of the more persistent and dramatic features of the data set [*Birkemeier*, 1984], and because it is well suited for a quantitative evaluation of the model. The topography near the bar was simple, the bar was outside of the surf zone, and the motion of the bar was qualitatively consistent with the behavior indicated by the model.

Application of the model requires estimates of the specific gravity and fall velocity of the sediment, the porosity of the sand bed, and time series of wave energy flux and low-frequency sea level fluctuations at an appropriate time interval (chosen here to be one hour). Comparison of model computations and field measurements requires determination of the cross-shore positions of depth contours of interest, and determination of the elevation and cross-shore position of the crest of the offshore bar. This section describes how we determined the required information from the reported measurements.

### 5.1 Beach Surveys

Figure 6 is a contour map of the Field Research Facility (FRF) of the Coastal Engineering Research Center. *Howd and Birkemeier* [1986] reported surveys on lines 58, 62, 188 and 190, indicated in the figure. The surveys shown in Figures 4 and 5 were obtained on lines 188 and 190, respectively. The datum for the surveys and for the tide gauge measurements (described below) is the National Geodetic Vertical Datum (NGVD).

*Howd and Birkemeier* [1986] reported 15 cross-shore surveys on lines 188 and 190 during the period of onshore bar

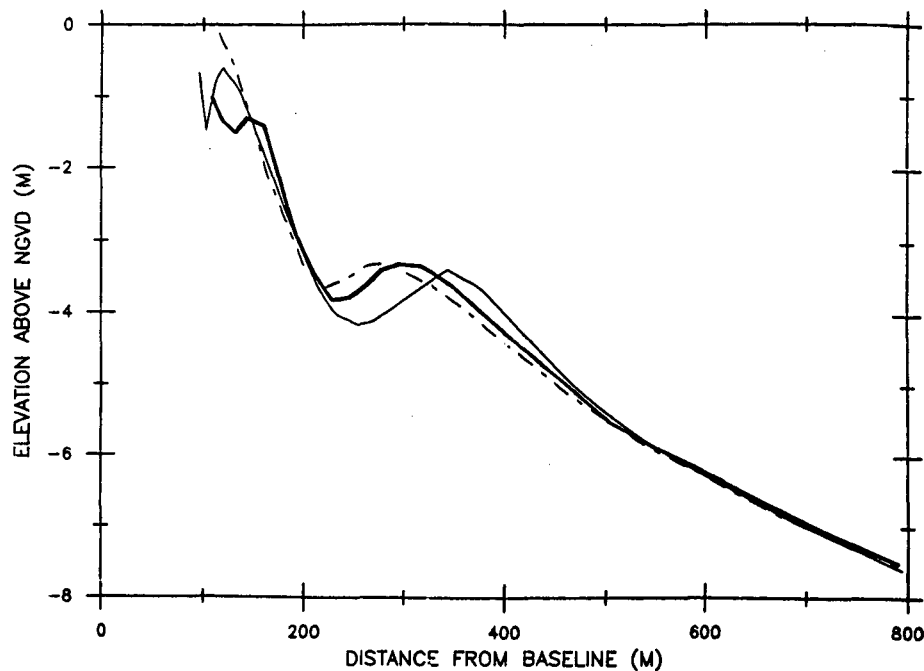


Fig. 5. Representative beach surveys along line 190 (see Figure 6) showing slow onshore motion of a long offshore bar. Light solid line: February 24, 1982; heavy solid line: May 17, 1982; dashed line: August 24, 1982.

movement (February 24, 1982 through August 24, 1982). We identified the position and elevation of the crest of the offshore bar in these surveys by fitting a quadratic curve through the three survey points nearest the bar crest, and by determining the position and elevation at which the quadratic curve had a relative maximum. We determined

the cross-shore positions of depth contours other than the crest by linear interpolation between the two nearest survey points bracketing the desired depth.

5.2. Wave and Tide Measurements

The U.S. Army Corps of Engineers maintains a wave staff and a tide gauge at the end of the FRF pier. A data logger samples the wave staff at 4 hz for 20 min bursts at intervals of 6 hours, reduced to intervals of 1 hour during storms, and a logger samples the tide gauge continuously at an interval of 6 min. The FRF staff provided records from the tide gauge and the wave staff for the period of interest to us.

The record from the tide gauge indicates periodic fluctuations associated with the astronomical tide, combined with significant subtidal fluctuations. The tide gauge record is of high quality, with a small number of clearly identified gaps. In order to produce a record of sea level fluctuations that could be used to apply our model, we used linear interpolation between the nearest adjacent data points to eliminate gaps. Linear interpolation is reasonable because the gaps are short (the longest is 1.5 hour and most are much shorter) and infrequent (there are only twenty gaps in the seven-month period between February and August 1982). We filtered the record in the time domain (using a triangular filter with a half-width of one hour) to remove low-energy fluctuations at high frequency, and we resampled the filtered record at an interval of one hour.

The record from the wave staff is also of high quality, with a few missing bursts and few bursts that appear, on the basis of visual inspection, to correspond to times when the wave staff was not operating correctly. Means of bursts obtained when the wave staff was operating correctly differ by a fairly constant offset from the surface elevation measured by the tide gauge, and we found that we could identify bad bursts in the wave staff record by examining means.

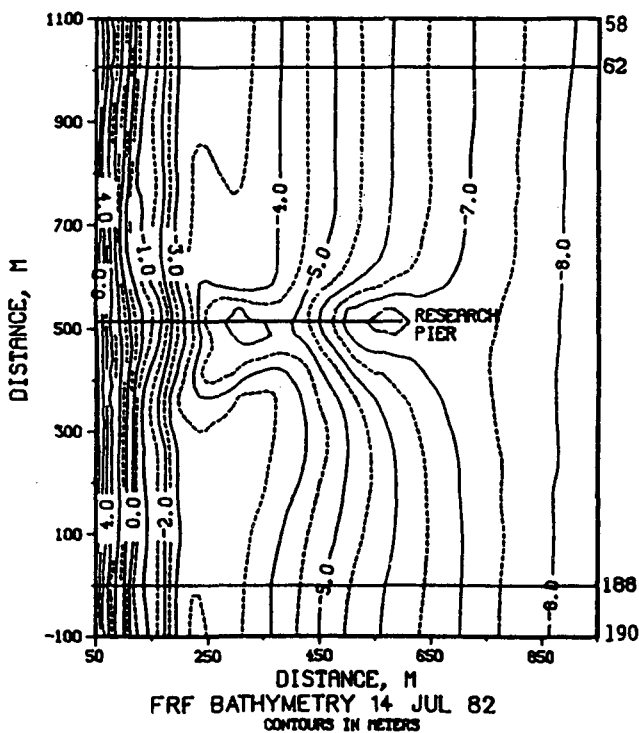


Fig. 6. Representative contour map of the Field Research Facility. The contours represent depth below NGVD in meters. The heavy line near the center is a pier. Reproduced from Howd and Birkemeier [1986].

To estimate the energy flux associated with each good data segment, we removed the mean, computed the power spectral density of the surface fluctuations (based on a record of 4096 points), smoothed the spectral estimates by averaging in the frequency domain (producing spectral estimates with 64 degrees of freedom), multiplied the smoothed spectral estimates at each frequency by the corresponding group velocity, and then integrated the result with respect to frequency. To calculate group velocities, we assumed that the depth below NGVD at the wave staff was 7.0 m, and we corrected the depth for low-frequency sea level fluctuations by using the processed tide gauge data. We found that estimates of energy flux are very insensitive to the degree of smoothing of the spectrum, and quite insensitive to the precise depth below NGVD at the wave staff.

We reduced the interval between estimates of energy flux to 1 hour, where necessary, by linear interpolation between estimates obtained from the wave staff records. The normalized autocovariance function computed from the time series of energy flux is high (above 0.90) at lags smaller than 10 hours, which indicates that linear interpolation is reasonable for the short intervals necessary (typically 6 hours). Linear interpolation was not necessary during storms, when the burst interval for the wave staff was 1 hour.

We did not incorporate refraction by small depth variations near the end of the FRF pier (see Figure 6) in our analysis of the wave data. Neglect of refraction is reasonable, because the depth contours offshore are fairly straight and parallel, and the waves propagate only a short distance through a region of irregular depth contours before reaching the wave staff. Our assumption of normal incidence at the pier end is necessary, because we do not have directional information, and it is also reasonable, because the wave staff is in relatively shallow water. Although the theoretical analysis presented in the preceding sections is based in part on linear long wave theory, we did not use long wave approximations in our calculation of energy flux at the wave staff, because the depth at the pier end (about 7.0 m) is significantly larger than typical depths near the crest of the offshore bar (about 3.5 m). Consequently dispersive effects may have been important at the pier end, while unimportant near the bar crest.

### 5.3. Sediment Characteristics

Howd and Birkemeier [1986] reported measurements of particle size distributions at several stations along line 188. Since our primary interest is modeling the evolution of the offshore bar, we chose to use the mean of the particle sizes measured at the three stations nearest the bar crest, which is 0.016 cm. Near the bar crest, the beach is composed primarily of quartz sand, with a specific gravity of approximately 2.65.

The sediment fall velocity depends on viscosity. During the period of interest to us, the water temperature at the FRF, and consequently the viscosity, varied. Although variations in fall velocity due to temperature changes may have been comparable to errors due to approximations made in the theoretical analysis, and uncertainty in the parameter  $Kf_w$ , we included the effect of temperature changes in our computations for the sake of completeness. The FRF staff provided daily measurements of water temperature, and we calculated the kinematic viscosity  $\nu$  by using the following

formula [e.g., White, 1979]:

$$\nu = \nu_o \exp[a + b(T_o/T) + c(T_o/T)^2] \quad (49)$$

Here  $T$  is absolute temperature,  $T_o$  is a reference temperature of 273.16 K,  $\nu_o$  is a reference viscosity of  $0.01792 \text{ cm}^2/\text{s}$ , and the constants  $a$ ,  $b$  and  $c$  are -1.94, -4.80 and 6.74, respectively. To calculate the fall velocity we used the following empirical expression for the drag coefficient for a sphere, suggested by Olson [see Graf, 1971]:

$$C_D = (24/Re)(1 + 3Re/16)^{1/2} \quad (50)$$

where  $C_D$  is the drag coefficient and  $Re$  is the Reynolds number, defined in the usual manner. Equation (50) is a good approximation for Reynolds numbers smaller than about 100. We used the daily measurements of water temperature to produce a time series of fall velocity, and we used linear interpolation to reduce the interval between estimates to one hour. As noted previously, the quantity  $Kf_w$ , considered here to be a constant, may in fact be a function of water and sediment properties, including in particular the kinematic viscosity. Because this possible functional dependence is unknown at present, we did not incorporate it into our calculations.

In our calculations we used a porosity  $n$  of 0.4, which is a reasonable value for a sand bed [e.g., Graf, 1971].

## 6. COMPARISON OF MEASUREMENTS AND MODEL COMPUTATIONS

### 6.1. Wave Breaking at the Crest of the Offshore Bar

Identification of periods during which wave breaking occurred near the crest of the offshore bar is necessary in order to interpret correctly a comparison of model computations and field measurements. Precise identification of periods of wave breaking is difficult. A parameter providing at least some information about breaking is the dimensionless root-mean-square (rms) surface displacement,  $[\langle \eta^2 \rangle]^{1/2}/h$ . Battjes [see Mei, 1982] collected laboratory measurements indicating that a ratio of wave height to water depth of very roughly 0.8 indicates onset of breaking on a plane beach. If the significant wave height is defined to be four times the rms surface displacement [e.g., Guza and Thornton, 1980], then this criterion corresponds to  $[\langle \eta^2 \rangle]^{1/2}/h$  equal to roughly 0.2. Guza and Thornton [1980] reported field measurements on a gently sloping beach indicating that well inside of the surf zone, the quantity  $[\langle \eta^2 \rangle]^{1/2}/h$  reaches a smaller constant value of approximately 0.1.

Figure 7 shows a time series of the dimensionless rms surface displacement at a depth  $H$  of 3.2 m, obtained by combining linear long wave theory with our estimates of energy flux and low frequency surface displacement, for the period of onshore bar motion identified by Birkemeier [1984]. A depth  $H$  of 3.2 m is the mean of the observed depths at the crest of the offshore bar along line 188 during this period. During most of the period of onshore bar motion, the dimensionless rms displacement was well below 0.2, suggesting that breaking probably did not occur near the bar crest. During an extreme event near the beginning of the record, however, the dimensionless rms displacement exceeded 0.2 by a considerable amount. Breaking probably occurred near the crest of the offshore bar during this event, and for this reason we do not consider the period before Julian day 60.

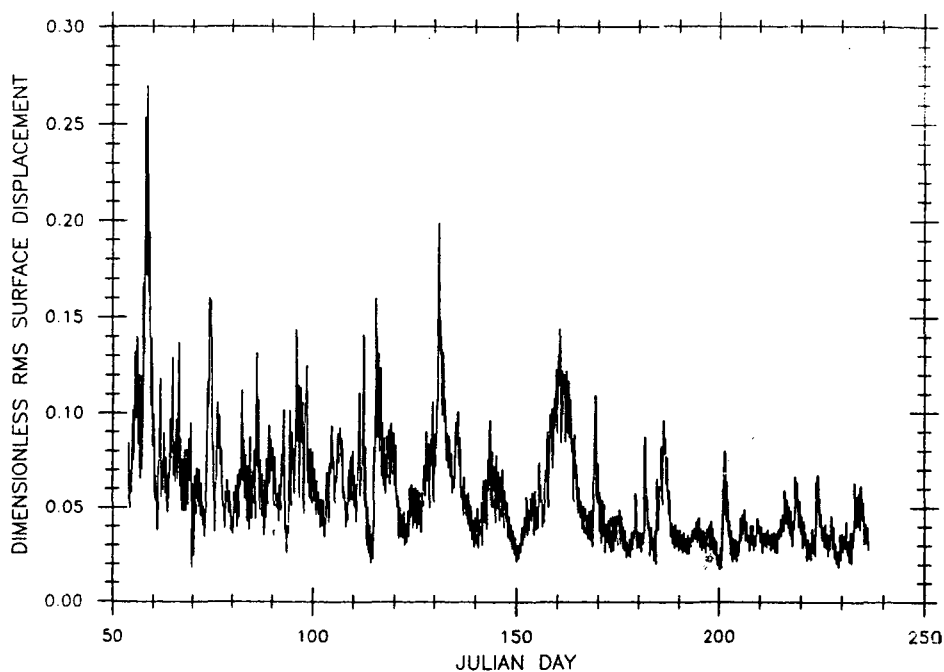


Fig. 7. Normalized root-mean-square surface displacement  $[\langle \eta^2 \rangle]^{1/2}/h$  at a depth below NGVD of 3.2 m (representative of the crest of the offshore bar on line 188).

A less severe event occurred on about day 130, during which the dimensionless rms surface displacement exceeded 0.2 by a slight amount, suggesting that breaking may have occurred near the bar crest.

6.2. Motion of the Crest of the Offshore Bar

According to (37) and (38), the elevation above a fixed datum at the crest of an offshore bar remains constant as the bar propagates onshore. If interpreted carefully, the

surveys reported by *Howd and Birkemeier* [1986] during the period of onshore bar motion are consistent with this theoretical result. Figure 8 shows estimates of the elevation above NGVD at the crest of the offshore bar along line 188, excluding the period before day 60. The elevation at the crest remained fairly constant but increased discernibly, and a standard statistical test for lack of correlation [e.g., *Benjamin and Cornell*, 1970], based on all of the data shown in Figure 8, indicates that we must reject at the 5% signifi-

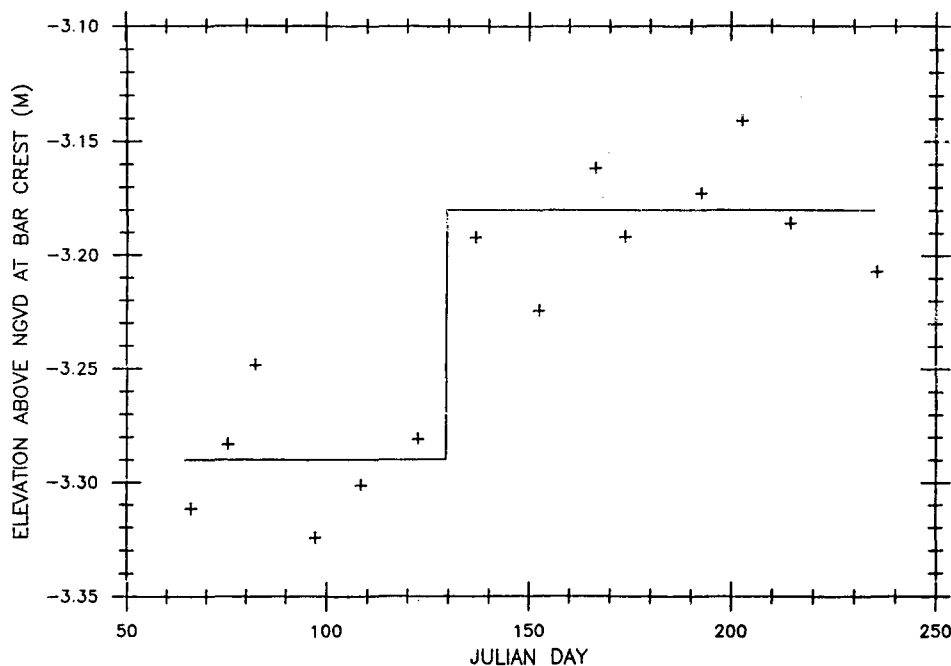


Fig. 8. Depth below NGVD at the crest of the offshore bar on line 188. Pluses: estimates based on the measurements reported by *Howd and Birkemeier* [1986]; solid lines: means of the data segments before and after day 130.

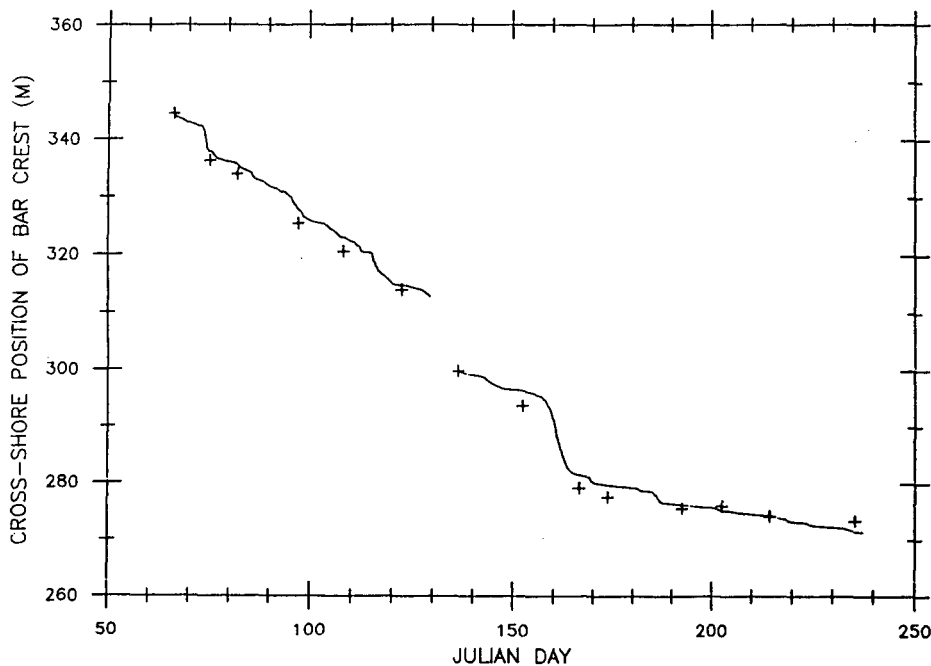


Fig. 9. Cross-shore position of the crest of the offshore bar on line 188. Pluses: estimates based on the measurements reported by *Howd and Birkemeier* [1986]; solid lines: Calculations based on (37) and (38) for the first and second segments of the data set (before and after day 130). For the first and second segments of the data set, the depths  $H$  at the bar crest used in the calculations were 3.29 and 3.18 m, respectively (see Figure 8).

cance level the null hypothesis that the crest elevation was linearly uncorrelated with time.

Close examination of Figure 8 reveals, however, that the period of onshore bar motion in fact consists of two segments, before and after day 130, during which the crest elevation was essentially constant. A statistical test for lack of correlation supports this observation, indicating that we can accept at the 5% significance level the null hypothesis that the crest elevation was linearly uncorrelated with time during each of the two segments, considered separately. Separate consideration of the two segments is reasonable, because breaking may have occurred near the crest of the offshore bar on about day 130, as noted above, and (37) and (38) apply only to unbroken waves. The essentially constant crest elevation observed during periods of unbroken waves, combined with the fact that down-slope shaking, as conventionally modeled, reduces the crest elevation (see section 4.3), suggests that down-slope shaking was not important near the crest of the offshore bar during the period of onshore bar motion. Estimates of the elevation of the crest of the offshore bar along line 190 support precisely the same conclusions, the only difference being that the crest elevation along line 190 was about 10 cm below the crest elevation along line 188.

Calculations of the position of the crest of the offshore bar based on (37) and (38) compare very well with observations. Figure 9 shows observations and calculations of the position of the crest of the offshore bar along line 188 for the first segment (before day 130) and the second segment (after day 130) of the period of onshore bar motion. The good agreement between model calculations and measurements shown in this figure suggests that the model represents realistically the sand transport and topographical changes that occurred near the crest of the offshore bar during the period

of onshore bar motion. A comparison of calculations and observations for line 190 shows very similar results.

### 6.3. Motion of Depth Contours Other Than the Crest

According to (37) and (38), two contours at the same depth on the landward and seaward slopes of an offshore bar propagate onshore at the same speed, in spite of the fact that the bottom slopes at the two contours are in general different. The measurements of onshore bar motion reported by *Howd and Birkemeier* [1986] are consistent with this theoretical result, if the depth contours are sufficiently near the crest of the offshore bar. The measurements indicate that further away from the crest, a contour at a given depth on the landward side of the bar propagates onshore at a slightly higher speed than a contour at the same depth on the seaward side of the bar.

Figure 10 shows the difference between the cross-shore positions of the two depth contours 3.4 m below NGVD on the seaward and landward slopes of the offshore bar along line 188. According to (37) and (38), this distance should be independent of time. Figure 10 shows that the period of onshore bar motion consists of two segments, before and after day 130, during which this distance was in fact essentially constant. For each of the two segments, a statistical test for lack of correlation indicates that we can accept at the 5% significance level the null hypothesis that the distance between the two depth contours was linearly uncorrelated with time. The behavior of the 3.4 m depth contours near the crest of the offshore bar along line 188 is therefore consistent with (37) and (38). As noted in section 4.3, down-slope shaking produces a slope-dependent correction to the onshore propagation speed, so that in general down-slope shaking would change the distance between the two depth contours. The

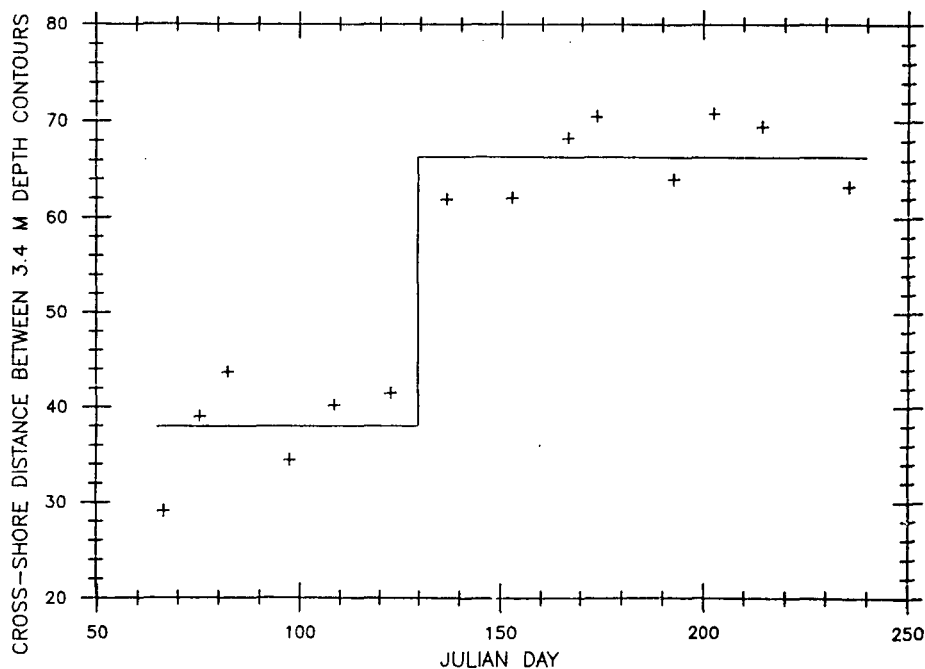


Fig. 10. Cross-shore distance between the 3.4 m contours on the seaward and landward slopes of the offshore bar on line 188. Pluses: estimates based on the measurements reported by *Howd and Birkemeier* [1986]; solid lines: means of the data segments before and after day 130.

essentially constant distance shown in Figure 10 during periods of unbroken waves suggests, as before, that down-slope shaking was not important near the crest of the offshore bar during the period of onshore bar motion.

The behavior of the 3.5 m depth contours on line 188 is different. Figure 11 shows the difference between the cross-shore positions of the two depth contours 3.5 m be-

low NGVD on the seaward and landward slopes of the offshore bar on line 188. Like Figure 10, Figure 11 shows an abrupt increase in the distance between the two contours on about day 130. Unlike Figure 10, however, Figure 11 suggests that the distance between the two contours gradually increased with time during the periods before and after 130. A statistical test for lack of correlation confirms this

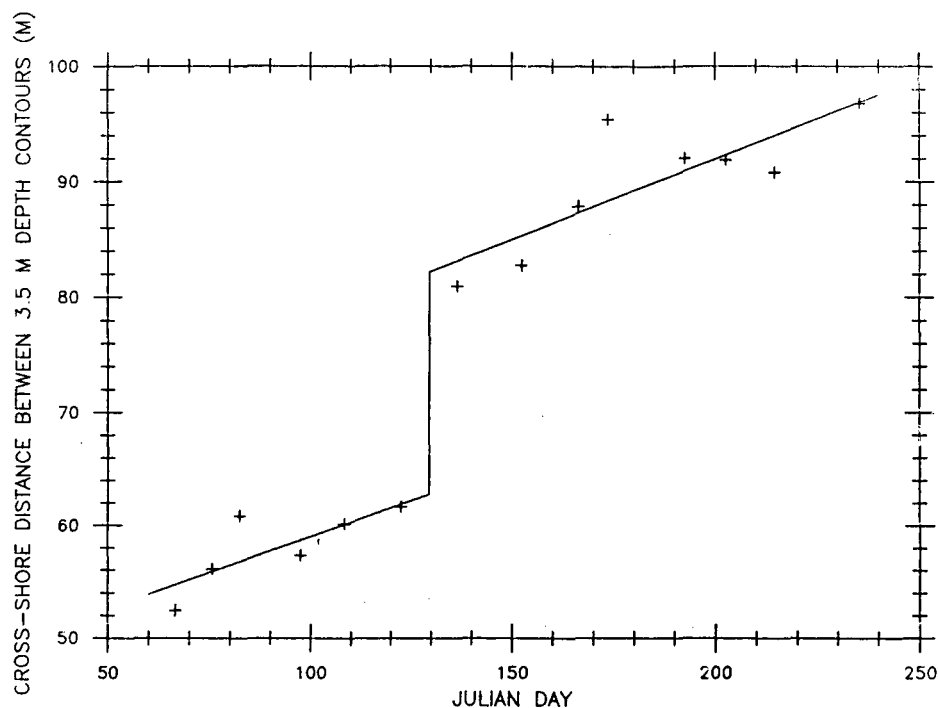


Fig. 11. Cross-shore distance between the 3.5 m contours on the seaward and landward slopes of the offshore bar on line 188. Pluses: estimates based on the measurements reported by *Howd and Birkemeier* [1986]; solid lines: least-squares straight-line fits to the measurements for the data segments before and after day 130.

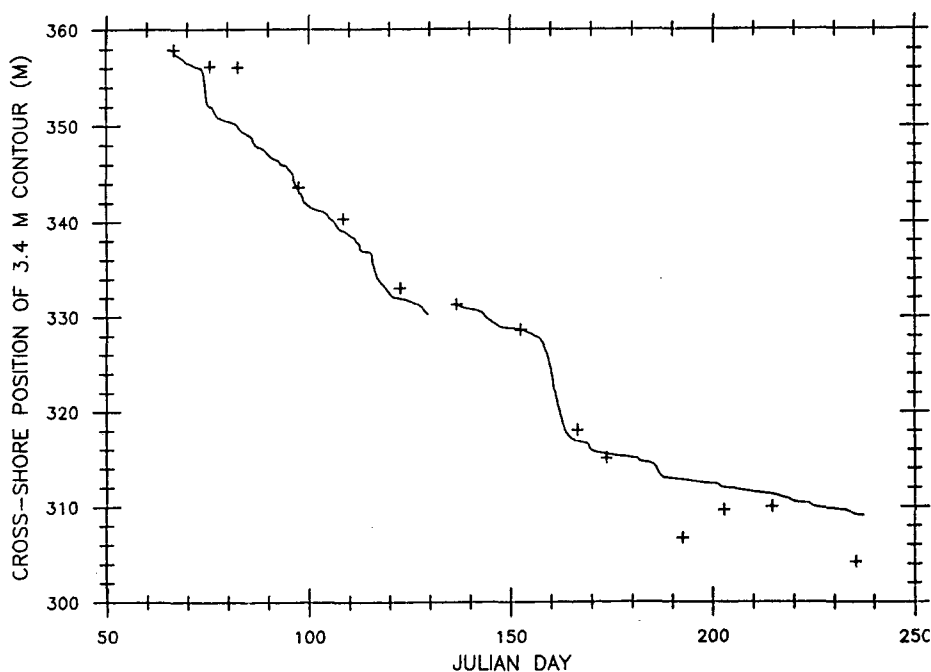


Fig. 12. Cross-shore position of the 3.4 m depth contour on the seaward side of the offshore bar on line 188. Pluses: estimates based on the measurements reported by *Howd and Birkemeier* [1986]; solid lines: calculations based on (37) and (38) for the first and second segments of the data set (before and after day 130).

visual impression, indicating that we must reject at the 5% significance level the null hypothesis that the distance was linearly uncorrelated with time during each of the two segments. Down-slope shaking may have increased the distance between the two depth contours during periods of unbroken waves, and some other process may also have contributed.

The discussion of topographical evolution along line 188 based on Figures 10 and 11 applies in precisely the same manner to topographical evolution along line 190. The only difference is that elevations along line 190 are about 10 cm lower than corresponding elevations along line 188. The comments that apply to the 3.4 and 3.5 m depth contours on line 188 apply without modification to the 3.5 and 3.6 m depth contours, respectively, on line 190.

In the neighborhood of an offshore bar on a beach, there are in general three contours at which the same depth occurs, if the depth is between the depth at the crest and the depth in the trough on the landward side of the bar (see, for example, Figures 4 and 5). According to (37) and (38), all three of these contours should propagate onshore at the same speed. Figures 10 and 11 and the accompanying discussion address only the two contours with the same depth on the seaward and landward slopes of the offshore bar, and do not address the third contour at the same depth, which is completely landward of the bar. The measurements reported by *Howd and Birkemeier* [1986] indicate that, in contrast to the theoretical prediction, this third contour remains at a nearly fixed position, and hardly propagates onshore at all. At present we do not have a satisfactory explanation of the nearly fixed position of the third contour, but we suspect that it may be due in part to the close proximity of the break point, which was typically roughly 200 m from the baseline during the period of onshore bar motion (see Figures 4 and 5), according to simplified calculations based on a constant ratio of wave height to water depth at break-

ing. Close proximity to the break point, where transport processes may vary rapidly in space, could have an important effect on the time history of the depth at a fixed point, because the time derivative of the depth is proportional to the spatial gradient of the transport rate (see (36)).

We did not carry out the kind of analysis shown in Figures 10 and 11 for contours at greater depths below NGVD. We could not obtain complete records of the position of contours at somewhat greater depths (for example, 3.6 m) on the landward slope of the offshore bar, because the trough on the landward side of the bar gradually filled with sand during the period of onshore bar motion (see Figures 4 and 5). Equations (37) and (38) do not describe this process. The gradual filling of the trough on the landward side of the bar was probably influenced strongly by the fact that contours completely landward of the bar remained at essentially fixed positions, as noted above, possibly due in part to the close proximity of the break point.

Calculations of the motion of depth contours near the crest of the offshore bar based on (37) and (38) agree very well with observations. Figure 12 shows calculations and observations of the position of the 3.4 m depth contour along line 188. As in Figure 9, the good agreement between model calculations and measurements suggests that the model represents realistically the sand transport and topographical changes that occurred sufficiently near the bar crest during the period of onshore bar motion. Calculations and observations of the position of the 3.5 m contour along line 190 show similarly good agreement.

Figure 13 shows a comparison of measurements and calculations of the position of the 5.0 m contour along line 188. We did not distinguish between the periods before and after day 130 in this calculation, because wave breaking probably did not occur near the 5.0 m contour during the extreme that took place on about day 130. The agreement between

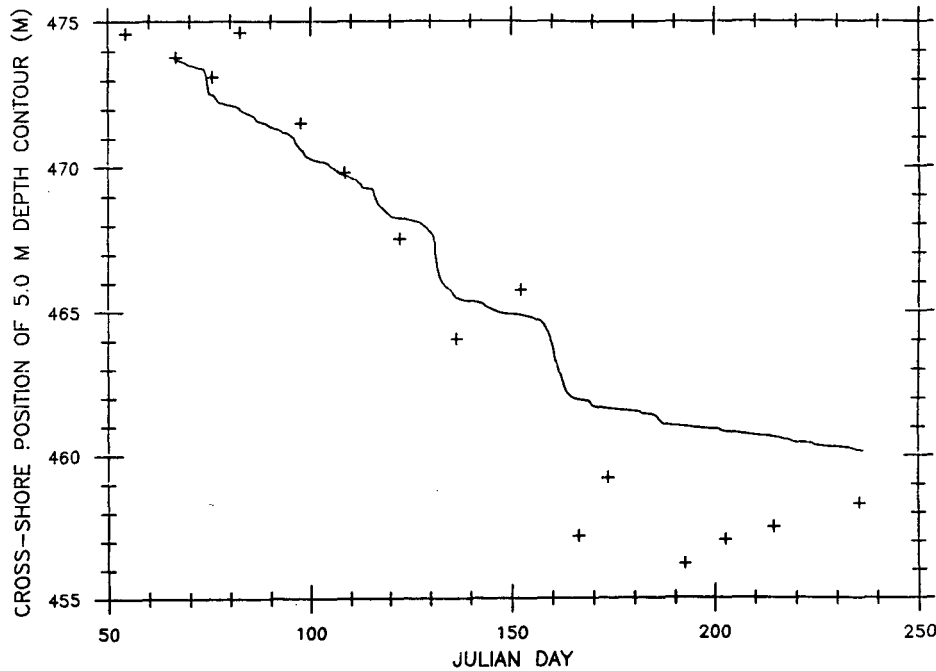


Fig. 13. Cross-shore position of the 5.0 m depth contour on line 188. Pluses: estimates based on the measurements reported by *Howd and Birkemeier* [1986]; solid line: calculation based on (37) and (38).

computations and measurements shown in Figure 13 is fairly good, although processes not included in the model, including in particular down-slope shaking, may have influenced sand transport at this depth, as was possibly the case with the 3.5 m contour. Comparison of Figures 9 and 13 shows an extreme reduction in the cross-shore propagation distance due to an increase in depth.

#### 6.4. Assessment of Model Assumptions

An important aspect of field application of a model is the question of whether the assumptions involved in the model development are justified in the field application. In the present case, the primary assumptions are that in the region of interest the depth contours are straight and parallel, the bottom slope is gentle, the waves are normally incident, unbroken and long, and sediment transport occurs as sheet flow. In addition, onshore transport by waves must be the dominant process producing topographical changes. Figures 4, 5 and 6, and the close correspondence between the topographical changes that occurred along lines 188 and 190 (noted above), indicate that the depth contours were in fact fairly straight and parallel near the crest of the offshore bar, and that the assumption of negligible alongshore variation is reasonable. We cannot evaluate the assumption of normally incident waves because of lack of directional information, although this assumption seems reasonable because of shallow depths. Section 6.1 addressed the question of wave breaking. This section addresses the remaining assumptions.

A simple order-of-magnitude analysis based on linear long wave theory suggests that local neglect of the effect of bottom slope on wave propagation requires that  $\partial_x(h)/(kh)$  be much smaller than unity. During the period of onshore bar motion, the wave period was of order 10 s, and straightforward calculations based on linear long wave theory demonstrate that in the neighborhood of the offshore

bar,  $\partial_x(h)/(kh)$  was in fact quite small. The portion of the beach landward of the point about 200 m from the baseline was much steeper than the offshore part of the beach, but the steep nearshore portion was inside or near the surf zone during the period of onshore bar motion, and is beyond the scope of the present study. Empirical values of the reflection coefficient for breaking waves on a plane sloping beach [e.g., *Mei*, 1982] suggest that during the period of onshore bar motion, wave reflection from the steep nearshore portion of the beach was quite weak.

A parameter indicating relative wave length is  $\omega_p(h/g)^{1/2}$ , where  $\omega_p$  is the radian frequency associated with the peak of the energy spectrum. For linear long waves,  $\omega_p(h/g)^{1/2}$  is equal to the product of water depth and wave number at the spectral peak, and a value less than 0.63 indicates that wavelengths in the energy-containing part of the spectrum are greater than about ten times the water depth. Our calculations indicate that about 95% of the crest movement shown in Figure 9 occurred during periods in which  $\omega_p(h/g)^{1/2}$  was less than 0.63, so that the assumption of long waves is realistic near the bar crest.

Several researchers have suggested empirical criteria for existence of oscillatory sheet flow. One of the more recent is the criterion presented graphically by *Shibayama and Horikawa* [1982], which corresponds to

$$\psi > 2.10(\theta^{-0.58}) \quad \psi > 269(\theta^{-2.57}) \quad (51)$$

where

$$\psi = f_w \langle U^2 \rangle / [gd(s-1)] \quad (52)$$

$$\theta = [2 \langle U^2 \rangle]^{1/2} / w_f \quad (53)$$

Here the wave friction factor is based on a boundary roughness equal to the mean grain diameter. The above criterion is based primarily on measurements in oscillatory flow at a

single frequency, but it presumably gives at least a crude indication of the existence of sheet flow under irregular waves. Calculations based on this criterion suggest that about 85% of the crest motion shown in Figure 9 occurred during periods in which sand was transported as sheet flow at the crest of the offshore bar. The assumption of sand transport as sheet flow is therefore reasonable.

It is difficult to demonstrate definitely that onshore transport by waves was the dominant process producing topographical changes near the crest of the offshore bar during the period of onshore bar motion. Competing effects may have included down-slope shaking, a mean alongshore transport rate that varied in the alongshore direction, and infragravity motions. As noted previously, the essentially constant crest elevation observed during periods of unbroken waves, and the lack of a slope-dependent effect on propagation speeds of contours sufficiently near the crest, suggest that down-slope shaking was not important near the crest of the offshore bar, although it clearly could have been important away from the crest. Neglect of an alongshore current and associated alongshore transport seems reasonable, because the primary effect driving an alongshore current (a breaking-induced cross-shore gradient in the radiation stress; see e.g., Mei [1982]) is not present well outside of the surf zone. In the absence of some other effect (such as a strong alongshore wind stress), it seems likely that bottom stresses and transport rates associated with alongshore currents were much smaller than bottom stresses and transport rates associated with incident waves. As noted in section 4.3, the possible role of infragravity motions is very difficult to assess at present, particularly in the absence of near-bottom velocity measurements.

## 7. SUMMARY AND CONCLUSIONS

This paper has presented a model of wave-induced sand transport and topographical changes seaward of the break point on a gently sloping beach, for the specific case in which the depth contours are straight and parallel, the waves are random, normally incident, weakly nonlinear, and relatively long, and the wave-induced motion is intense enough so that the bottom boundary layer is turbulent, and sand transport occurs as sheet flow. The model consists of four components: (1) a new empirical expression for sand transport as sheet flow, in which the instantaneous transport rate is directly proportional to the instantaneous bottom shear stress; (2) an expression for the mean bottom shear stress in a wave-induced flow field, which follows from a theoretical analysis of the mean momentum balance in the bottom boundary layer; (3) a simple representation of the shoaling random wave field, in which the probability density function of the surface displacement is Gaussian, linear long wave theory describes the local structure of the waves, and the waves conserve energy flux as they shoal; and (4) the equation for conservation of sediment mass. Because the model represents only one process (sand transport due to a mean bottom stress) and because it applies only under a specific set of conditions, the model always indicates onshore transport, and it indicates that depth contours move onshore at a speed that depends only on the incident wave conditions, the sand properties, and the local depth. The model applies only to situations very far from a possible equilibrium configuration,

in which onshore sand transport by waves balances offshore transport by some other process.

This paper has also presented a comparison of model calculations with field measurements of topographical changes presented by Birkemeier [1984] and reported in detail by Howd and Birkemeier [1986]. The comparison addressed a six-month period during which a prominent offshore bar moved a significant distance onshore. The model reproduces very well the motion of the crest of the offshore bar and the motion of contours near the crest. Calculations of the motion of contours further away from the crest are less satisfactory, but still reasonable. Processes not included in the model, such as down-slope shaking due to the direct influence of gravity on the transport process, may have had a significant impact on topographical changes away from the crest. Most of the special conditions required by the model appear to have been satisfied reasonably well near the crest of the bar during most of the period of onshore bar motion, although we could not address in a definite manner the possible roles of transport processes not included in the model (including transport associated with infragravity motions).

The surprisingly good agreement between model computations and field measurements must to some extent be regarded as fortuitous, because of the simplicity of the model and the number of processes neglected. In addition, favorable comparison with a single field data set is not strong support for any model of sand transport by water waves. Because of the amount of time required to carry out a detailed comparison of model computations and field measurements, we have not examined other field data sets, or other segments of the Birkemeier-Howd data set.

On the other hand, it is interesting that a model based on straightforward ideas (proportionality between sand transport rate and bottom shear stress, a simple mean momentum balance in the bottom boundary layer, and a simple representation of the shoaling random wave field) can reproduce field measurements of topographical changes on beaches, without empirical tuning, under conditions in which the model is believed to apply. The favorable agreement between model calculations and field measurements is encouraging, and suggests that the separate components of the model may be fairly realistic. The approach presented here may possibly be used in other applications to provide insight into sand transport processes on beaches.

*Acknowledgments.* This publication is a result of research sponsored by the National Science Foundation (grants CEE-8404258 and OCE-87-10768) and National Oceanic and Atmospheric Administration (NOAA) Office of Sea Grant, Department of Commerce (grants NA85AA-D-SG033 and NA86AA-D-FG090). The field measurements used in this paper were made available through the Measurements and Analysis Program of the U.S. Army Engineer Waterways Experiment Station's Coastal Engineering Research Center's Field Research Facility. We thank in particular W. Birkemeier and M. Leffler, of the Field Research Facility, for their cooperation. We are grateful to N. Kobayashi for constructive comments during the initial phase of the research, and to O. S. Madsen for comments on an early draft of the manuscript. This is contribution number 6754 from the Woods Hole Oceanographic Institution.

## REFERENCES

- Ahilan, R. V., and J. F. A. Sleath, Sediment transport in oscillatory flow over flat beds, *J. Hydraul. Eng.*, 113, 308-322, 1987.
- Bagnold, R. A., Mechanics of marine sedimentation, in *The Sea*,

- vol. 3, edited by M. N. Hill, pp. 507-528, Interscience, New York, 1963.
- Bailard, J. A., An energetics total load sediment transport model for a plane sloping beach, *J. Geophys. Res.*, *86*, 10938-10954, 1981.
- Bailard, J. A., and D. L. Inman, An energetics bedload model for a plane sloping beach: Local transport, *J. Geophys. Res.*, *86*, 2035-2043, 1981.
- Battjes, J. A., Surf zone hydrodynamics, *Annu. Rev. Fluid Mech.*, *20*, 257-294, 1988.
- Benjamin, J. R., and C. A. Cornell, *Probability, Statistics, and Decision for Civil Engineers*, McGraw-Hill, New York, 1970.
- Benjamin, T. B., B. Boczar-Karakiewicz, and W. G. Pritchard, Reflection of water waves in a channel with corrugated bed, *J. Fluid Mech.*, *185*, 249-274, 1987.
- Birkemeier, W. A., Time scales of profile change, in *Proceedings of the 19th Coastal Engineering Conference*, pp. 1507-1521, American Society of Civil Engineers, New York, 1984.
- Bowen, A. J., Simple models of nearshore sedimentation: Beach profiles and longshore bars, *The Coastline of Canada*, edited by S. McCann, *Pap. 80-10*, pp. 1-11, Geol. Surv. of Can., Ottawa, 1980.
- Bowen, A. J., and D. A. Huntley, Waves, long waves and nearshore morphology, *Mar. Geol.*, *60*, 1-13, 1984.
- Carter, T. G., P. L. F. Liu, and C. C. Mei, Mass transport by waves and offshore sand bedforms, *J. Waterw., Port Coastal Ocean Div. Am. Soc. Civ. Eng.*, *99*, 165-184, 1973.
- Dally, W. R., and R. G. Dean, Suspended sediment transport and beach profile evolution, *J. Waterw., Port Coastal Ocean Div. Am. Soc. Civ. Eng.*, *110*, 15-33, 1984.
- Dean, R. G., and R. A. Dalrymple, *Water Wave Mechanics for Engineers and Scientists*, Prentice-Hall, Englewood Cliffs, N. J., 1984.
- Draper, N. R., and H. Smith, *Applied Linear Regression*, John Wiley, New York, 1966.
- Elgar, S., and R. T. Guza, Shoaling gravity waves: Comparisons between field observations, linear theory, and a nonlinear model, *J. Fluid Mech.*, *158*, 47-70, 1985.
- Elgar, S., and R. T. Guza, Nonlinear model predictions of bispectra of shoaling surface gravity waves, *J. Fluid Mech.*, *167*, 1-18, 1986.
- Foda, M. A., and C. C. Mei, Nonlinear excitation of long trapped waves by a group of short swells, *J. Fluid Mech.*, *111*, 331-345, 1981.
- Freilich, M. H., and R. T. Guza, Nonlinear effects on shoaling surface gravity waves, *Philos. Tran. R. Soc. London, Ser. A*, *311*, 1-41, 1984.
- Graf, W. H., *Hydraulics of Sediment Transport*, McGraw-Hill, New York, 1971.
- Grant, W. D., and O. S. Madsen, Movable bed roughness in unsteady oscillatory flow, *J. Geophys. Res.*, *87*, 469-481, 1982.
- Grant, W. D., and O. S. Madsen, The continental shelf bottom boundary layer, *Annu. Rev. Fluid Mech.*, *18*, 265-305, 1986.
- Guza, R. T., and E. B. Thornton, Local and shoaled comparisons of sea surface elevations, pressures and velocities, *J. Geophys. Res.*, *85*, 1524-1530, 1980.
- Guza, R. T., and E. B. Thornton, Velocity moments in nearshore, *J. Waterw., Port Coastal Ocean Div. Am. Soc. Civ. Eng.*, *111*, 235-256, 1985.
- Hallermeier, R. J., Oscillatory bedload transport: Data review and simple formulation, *Continental Shelf Res.*, *2*, 159-190, 1982.
- Heathershaw, A. D., Seabed-wave resonance and sand-bar growth, *Nature*, *296*, 343-345, 1982.
- Heathershaw, A. D., and A. G. Davies, Resonant wave reflection by transverse bedforms and its relation to beaches and offshore bars, *Mar. Geol.*, *62*, 321-338, 1984.
- Holman, R. A., Edge waves and the configuration of the shoreline, in *Handbook of Coastal Processes and Erosion*, edited by P. Komar, pp. 21-33, CRC Press, Boca Raton, Fla., 1983.
- Holman, R. A. and A. J. Bowen, Bars, bumps and holes: Models for the generation of complex beach topography, *J. Geophys. Res.*, *87*, 457-468, 1982.
- Horikawa, K., Coastal sediment processes, *Annu. Rev. Fluid Mech.*, *13*, 9-32, 1981.
- Horikawa, K., A. Watanabe, and S. Katori, Sediment transport under sheet flow condition, in *Proceedings of the 18th Coastal Engineering Conference*, pp. 1335-1352, American Society of Civil Engineers, New York, 1982.
- Howd, P. A., and W. A. Birkemeier, Beach and nearshore survey data: 1981-1984, CERC Field Research Facility, Technical Report, Dept. of the Army, U.S. Army Corps of Eng., Waterw. Exp. Stn., Vicksburg, Miss., 1986.
- Hunt, J. N., and B. Johns, Currents produced by tides and gravity waves, *Tellus*, *15*, 343-351, 1963.
- Jonsson, I. G., Wave boundary layers and friction factors, *Proceedings of the 10th Coastal Engineering Conference*, pp. 127-148, American Society of Civil Engineers, New York, 1966.
- Jonsson, I. G., A new approach to oscillatory rough turbulent boundary layers, *Ocean Eng.*, *7*, 109-152, 1980.
- Jonsson, I. G., and N. A. Carlsen, Experimental and theoretical investigations in an oscillatory turbulent boundary layer, *J. Hydraul. Res.*, *14*, 45-60, 1976.
- Kajiura, K., A model of the bottom boundary layer in water waves, *Bull. Earthquake Res. Inst.*, *46*, 75-123, 1968.
- Kobayashi, N., Sediment transport on a gentle slope due to waves, *J. Waterw., Port Coastal Eng. Div. Am. Soc. Civ. Eng.*, *108*, 254-271, 1982.
- Komar, P. D., and R. A. Holman, Coastal processes and the development of shoreline erosion, *Annu. Rev. Earth Planet. Sci.*, *14*, 237-265, 1986.
- Lau, J., and B. Travis, Slowly varying Stokes waves and submarine longshore bars, *J. Geophys. Res.*, *78*, 4489-4497, 1973.
- Lavelle, J. W., and H. O. Mofjeld, Effects of time-varying viscosity on oscillatory turbulent channel flow, *J. Geophys. Res.*, *88*, 7607-7616, 1983.
- Lighthill, M. J., and G. B. Whitham, On kinematic waves, 1, Flood movement in long rivers, *Proc. R. Soc. London, Ser. A*, *229*, 281-316, 1955.
- Longuet-Higgins, M. S., The mechanics of the boundary layer near the bottom in a progressive wave, in *Proceedings of the 6th Coastal Engineering Conference*, pp. 184-193, American Society of Civil Engineers, New York, 1958.
- Madsen, O. S., and W. D. Grant, Sediment Transport in the Coastal Environment, *Rep. 209*, Ralph M. Parsons Lab. for Water Resour. and Hydrodyn., Mass. Inst. of Technol., Cambridge, 1976a.
- Madsen, O. S., and W. D. Grant, Quantitative description of sediment transport by waves, in *Proceedings of the 15th Coastal Engineering Conference*, pp. 1093-1112, American Society of Civil Engineers, New York, 1976.
- Manohar, M., Mechanics of bottom sediment movement due to wave action, *Tech. Memo. 75*, Beach Erosion Board, Office of the Chief of Eng., Dept. of the Army, Vicksburg, Mississippi, 1955.
- Mei, C. C., *The Applied Dynamics of Ocean Surface Waves*, McGraw-Hill, New York, 1982.
- Mei, C. C., Resonant reflection of surface water waves by periodic sandbars, *J. Fluid Mech.*, *152*, 315-336, 1985.
- Mizuguchi, M., and M. Mori, Modeling of two-dimensional beach transformation due to waves, *Coastal Eng. Jpn.*, *24*, 155-170, 1981.
- Nielsen, P., Three simple models of wave sediment transport, *Coastal Eng.*, *12*, 43-62, 1988.
- Nishimura, H., and Sunumura, T., Numerical simulation of beach profile changes, *Proceedings of the 20th Coastal Engineering Conference*, pp. 1444-1455, American Society of Civil Engineers, New York, 1986.
- Sallenger, A. H., and Holman, R. A., Infragravity waves over a natural barred profile, *J. Geophys. Res.*, *92*, 9531-9540, 1987.
- Sawamoto, M., and T. Yamashita, Sediment transport rate due to wave action, *J. Hydraul. Eng.*, *4*, 1-15, 1986.
- Shibayama, T., and K. Horikawa, Bed load measurement and prediction of two-dimensional beach transformation, *Coastal Eng. Jpn.*, *23*, 179-190, 1980.
- Shibayama, T., and K. Horikawa, Sediment transport and beach transformation, in *Proceedings of the 18th Coastal Engineering Conference*, pp. 1439-1458, American Society of Civil Engineers, New York, 1982.
- Short, A. D., Multiple offshore bars and standing waves, *J. Geophys. Res.*, *80*, 3833-3840, 1975.
- Stive, M. J. F., A model for cross-shore sediment transport, in

- Proceedings of the 20th Coastal Engineering Conference*, pp. 1550-1564, American Society of Civil Engineers, New York, 1986.
- Stive, M. J. F., and J. A. Battjes, A model for offshore sediment transport, in *Proceedings of the 19th Coastal Engineering Conference*, pp. 1420-1436, American Society of Civil Engineers, New York, 1984.
- Sunumura, T., A laboratory study of offshore transport of sediment and a model for eroding beaches, in *Proceedings of the 17th Coastal Engineering Conference*, pp. 1051-1069, American Society of Civil Engineers, New York, 1980.
- Symonds, G., and A. J. Bowen, Interactions of nearshore bars with incoming wave groups, *J. Geophys. Res.*, 89, 1953-1959, 1984.
- Townsend, A. A., *The Structure of Turbulent Shear Flow*, Cambridge University Press, New York, 1976.
- Trowbridge, J. H., and O. S. Madsen, Turbulent wave boundary layers, 1, Model formulation and first-order solution, *J. Geophys. Res.*, 89, 7989-7997, 1984.
- White, F. M., *Fluid Mechanics*, McGraw-Hill, New York, 1979.
- 
- J. Trowbridge, Woods Hole Oceanographic Institution, Woods Hole, MA 02543.
- D. Young, U.S. Army Corps of Engineers, Los Angeles, CA 91306.

(Received April 25, 1988;  
revised November 9, 1988;  
accepted February 14, 1989.)